Time-Frequency Analysis of the Auditory Brainstem Response

Henrik Johansson F09, 910730

October 14, 2013

Acknowledgements

I would like to thank my supervisor Maria Sandsten for her great support and guidance. Her ideas and helpful advice have been invaluable. Most of my work has been done at the Centre of Mathematical Sciences at Lund Institute of Technology from April through summer and early autumn. I would also like to thank SensoDetect AB, and Johan Källstrand in particular for giving me data to analyse.

Abstract

This thesis is about time-frequency analysis of the brainstem auditory evoked potential (BAEP). The work can be divided into two parts. One part where a model is built up from a very simple example to a more complex model resulting in a model consisting of a sum of sinusoids with stochastic starting points and amplitudes. Different time-frequency methods have been evaluated for these models and the multi window spectrogram with Hermitian base functions performs the best in a real life situation with more than one component and a high level of noise.

The second part consists of investigating real BAEP data. BAEP data from five patients were available. Each patient has two data sets which have been studied. One while the patient is awake and one while it is asleep. A hypothesis is that there exists some sort of difference between these two datasets. It turns out that it does. The earlier peaks differ slightly in latency and the later peaks for the sleeping data seem to disappear. This result is concluded from different time frequency methods, where the spectrogram and the multi-window spectrogram are the most successful methods. An attempt to make a bootstrap simulation in order to estimate the mean and confidence bounds of each peak is also made for one dataset.

Contents

Chapter 1

Introduction

1.1 Purpose

The purpose of this work has been to investigate the brainstem auditory evoked potentials (BAEP) with a series of tools from time-frequency analysis. As of today there has not been a lot of research conducted on this type of brain signal from a signal processing perspective. However, it has been shown that the BAEP is a useful tool for diagnosing a series of grave psychiatric disorders, such as Schizophrenia and ADHD [6]. A company from Lund, called SensoDetect AB, has specialized in this type of diagnostics.

However, it is clear that the signal is non-stationary and very noisy. Because of this we suspect that there is information which can be extracted through the use of time-frequency analysis. Two different approaches have been applied to investigate the BAEP. One approach was to get a feeling for the BAEP and it's properties in the time-frequency domain from real data supplied by SensoDetect AB. A further step was to try to investigate if there appears a difference between data recorded from a sleeping subject during operation and data from the same subject recorded while the subject was awake. We suspect that there might be a latency shift, which has been found for the mid-latency evoked potential [5]. The goal of the second approach was to become familiar with common models and methods used in time-frequency analysis.

A limitation has been set with respect to the data gathered from SensoDe-

tect AB. SensoDetect AB is developing an objective diagnostic method for psychiatric diseases such as schizophrenia and ADHD [6]. According to their studies, their method has over 80% sensitivity. The pre-processing of the data has not been looked into at all. From a signal processing perspective, there could be many ways of improving and smoothing the data which SensoDetect do not explore. Because of some difficulties regarding acquisition of data and also limited time, this avenue was not pursued.

1.2 Outline

The outline of the report looks as follows. At first a background is given of the Evoked Potential(EP) in general and the Brainstem Auditory Evoked Potential (BAEP) in particular. It continues with a rather thorough theoretical part, which handles the mathematical theory and concepts which lie as a foundation of the report. The various time-frequency tools are presented here and also the mathematics building up to them. After that a number of different mathematical models are shown and different time-frequency tools are tested to see how they perform for different types of models. Under the result part, the results from investigating the real data are shown. The report is wrapped up by a discussion of issues encountered along the way and ways to continue the work.

1.3 Evoked Potentials

Evoked potentials are event related activity which occurs as electrical response from the brain or the brainstem. A variety of types of sensory stimulation exist, but auditory and visual stimulation are the most commonly used. This report will be fully focused on auditory evoked potentials. The recording of these signals provide a non invasive diagnostic tool. This means that you do not have to operate on the subject to diagnose him. Instead you measure the EP through electrodes on the scalp in a set up similar to that of an ECG recording. The evoked potentials can give information on for example sensory pathway abnormalities, localization of lesions affecting the sensory pathways and disorders related to language and speech. It can also be used during surgery, both to monitor the depth of anaesthesia [5] and in order to see that no neural paths has been damaged. The potentials

manifest themselves as a transient waveform whose morphology depends on the type and strength of the stimulus. The mental state of the subject: the subject's attention, wakefulness and expectation for example, also influence the waveform morphology [3].

Figure 1.1: The figure shows the SensoDetect measurement set-up. Five electrodes are placed on the subjects scalp. Two behind the ears and three in the forehead. The subject then puts on a set of headphones, which play a click sound. The electrodes then measure the EP. The measurement session is conducted while the subject is simply sitting down in a chair in a dark, quiet room. Printed with permission from SensoDetect AB.

Auditory EP are generated in response to an auditory stimulation. In this case the generated sound is a short click, which is heard through headphones. The click is produced by a 0.1 ms square wave pulse, with a repetition rate of 8-10 clicks per second. Individual evoked potentials have a very low amplitude, ranging from 0.1μV to 10μV, this means that the individual EP are subject to a high noise level. However, as the response usually occurs after a given time, in this case a few milliseconds, after stimulus, one can deal with the noise with various signal processing techniques. Ensemble averaging is one way. Practically it means that around 1000 stimuli are averaged to cancel out the noise and to get a consistent waveform. When the noise has been

reduced, the latency and amplitude of each constituent wave for the EP can be estimated and interpreted in clinical terms.

Although the AEP consists of several parts, the focus lies in the BAEP in this report. The BAEP has a very low amplitude, from 0.1 to 0.5 μV, and occurs from 2 to 12 ms after stimulus. The BAEP consists of up to seven waves in a normal subject and is shown in figure 1.2. The waves are labelled with Roman numbers. The loss or reduction of individual waves provides clinically important information, as does the absolute latency and the inter-peak latency. The characteristics of these waveforms in the spectral domain are studied closely in this report.

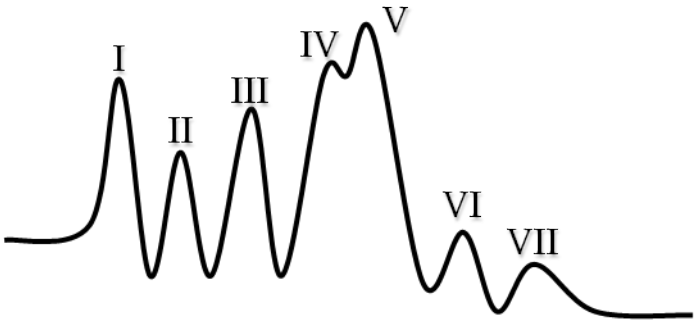

Figure 1.2: The figure shows the BAEP waveform. The waves labelled with Roman numbers.

1.4 Pre-Processing of Data

The data used in this thesis was BAEP data from five subjects. For four of the subjects, both awaken data, pre-operation, and sleeping data, during operation, was available. For one subject, only the awaken data was available. The data was given in the form of an excel file which was later converted into a MATLAB file so that it could be studied with time-frequency tools. The raw data was obtained by sampling the evoked potential 256 times over 15 ms. This was repeated roughly 1300 times. SensoDetect perform several steps of signal processing. They convert their data from hexadecimal form to decimal forms, find and eliminate spikes, remove the 50 Hz interference,and take a smoothing moving average among other things. They also average 30 consecutive EP, with an overlap of 15. This average is what is studied in the report. The difference between taking an average in time and then transforming into the spectral domain and taking an average of data after it has been transformed into the spectral domain is investigated.

Chapter 2

Theoretical Concepts and Methods

2.1 Stationary Stochastic Processes

The starting point for analysing a signal is to look into stochastic processes. Most theory and most methods rely on the assumption of a stationary stochastic process. In signal processing applications one is usually satisfied with something referred to as a weakly stationary stochastic process (WSS). A WSS process has a constant mean function $m(t)$ and the covariance function $r(s,t)$ is everywhere finite, and depends only on the time difference $\tau = t - s$ [7]. The power spectral density (PSD) of a process is defined as

$$S_x(f) = \int_{-\infty}^{\infty} r_x(\tau) e^{-i2\pi f\tau} d\tau. \tag{2.1}$$

There exists a plethora of methods for analysing a stochastic process. Almost all of them rely on the assumption above. The different methods can be categorised into parametric methods and non-parametric methods. Parametric methods are usually based on the auto regressive moving average (ARMA) model

$$x_t + a_1 x_{t-1} + ...a_p x_{t-p} = e_t + c_1 e_{t-1} + ...c_q e_{t-q} \tag{2.2}$$

of order AR(p) and MA(q).

Parametric methods generally rely on forehand information of a process being available. This thesis will not handle parametric methods, but instead focus on non-parametric methods. The strength of non-parametric methods lies in that they usually require no forehand knowledge of the signal and this is the case for the signals studied in this thesis.

2.2 Spectral Analysis

When analysing a signal or a stochastic process, it is of great use to study the signal not only in the time domain, but also in the frequency (spectral) domain. The cornerstone of spectral analysis is the Fourier transform, which transforms the signal from the time domain to the frequency domain. There is often a lot of useful information in this domain, which cannot be found without further investigation. Because of this there exists an abundance of different methods and theories developed in order to analyse the spectral content of a signal or a stochastic process.

2.3 Periodogram

Non-parametric methods are usually based on the periodogram, an estimate of the spectral density for the process. As real data are studied, it follows that the data has to be sampled. Hence the discrete Fourier transform is of interest. Assume that one has N samples of the signal x(n), where $0 \leq$ n $\leq$ N-1. The discrete Fourier transform (DFT) X(f) of x(n) is then found as

$$X(f) = \sum_{n=0}^{N-1} x(n) e^{-i2\pi fn}. \tag{2.3}$$

This leads straight to the periodogram, which was one of the earliest ways to estimate the frequency content of a signal. The periodogram is defined as the squared absolute value of the DFT [8],

$$\hat{S}_x(f) = \frac{1}{N} \left| \sum_{n=0}^{N-1} x(n) e^{-i2\pi fn} \right|^2 = \sum_{\tau-N+1}^{N-1} \hat{r}_x(\tau) e^{-i2\pi\tau}, \tag{2.4}$$

where $\hat{r}_x(\tau)$ is the estimate of the covariance funtion defined as,

$$\hat{r}_x(\tau) = \frac{1}{N} \sum_{n=0}^{N-1-|\tau|} x(n)x(n+\tau). \tag{2.5}$$

It is important that the analysed signal is WSS, as the periodogram is not able to capture frequency content which changes over time. The periodogram gives a first estimate of the PSD. The estimate suffers from a couple of problems. Among them being that the variance does not decrease with the number of data samples and the occurrence of spectral leakage, which gives bad resolution.

2.4 Welch's Method and Multitapers

In order to reduce the variance and bias of the periodogram, Welch developed a method which consists of measuring the PSD of subsets of the data set, rather than of the entire set of data. These subsets may overlap and an overlap of 50% is common. The final estimate of the PSD will then be the mean of the PSD of the subsets. One way to visualize the method is to imagine a sliding window in time, which measures the PSD at every step. This method decreases the variance of the PSD estimate and the variance also decreases with the number of averages.

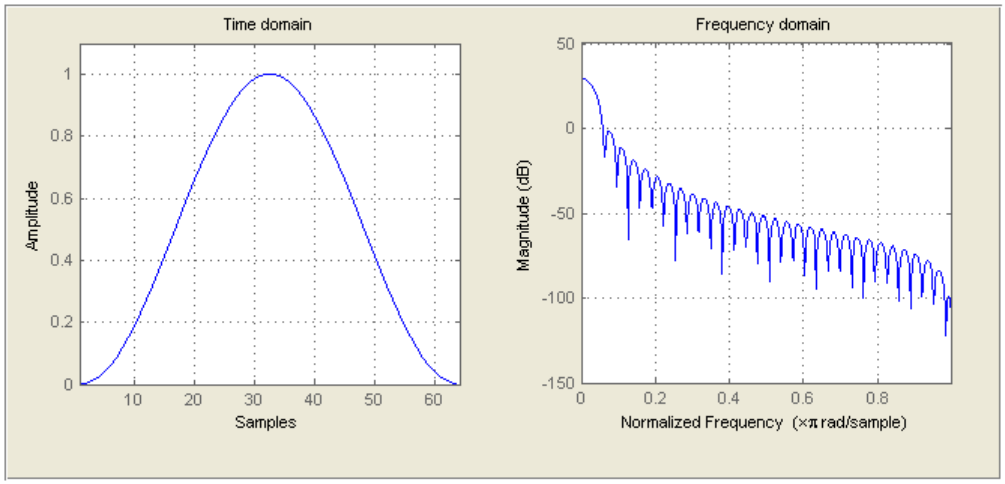

Figure 2.1: The figure shows the Hanning window in both the time and frequency domains.

The windowed periodogram is introduced as

$$\hat{S}_x(f) = |\sum_{n=0}^{N-1} w(n)x(n)e^{-i2\pi fn}|^2 \tag{2.6}$$

where $w(n)$ is a window or taper [8]. The important properties of a window varies with the application. Preferably one would like a window which gives a narrow main lobe yielding a high resolution and low power side-lobes to avoid leakage, but normally there is a trade-off between resolution and spectral leakage. There is a large variety of different windows, but the one used mostly in this report is the Hanning window, which is shown in figure 2.1.

The concept of multi-tapers builds on Welch's method. The main idea of multi-tapers is reducing the variance of the periodogram, by using an average over several periodograms. However, to reach this reduction in variance, the periodograms have to be uncorrelated. This is achieved through the Welch method, by using the same window for all periodograms, but shifting it in time, which results in uncorrelated periodograms. If one instead uses orthogonal windows one can use the entire data set and the periodograms will still be uncorrelated. When producing multi-taper estimates of a spectrum

from N samples of a discrete-time random process $x(n)$ one averages over K periodograms.

$$\hat{S}(f) = \sum_{k=1}^{K} \alpha_k \hat{S}_k(f), \tag{2.7}$$

where α_k is a weighting factor and

$$\hat{S}_k(f) = |\sum_{n=0}^{N-1} x(n) h_k(n) e^{-i2\pi fn}|^2. \tag{2.8}$$

Here, $h_k(n) = [h_k(0)...h_k(N-1)]^T$, is the k:th data window in the set $k = 1...K$.
In this report, a method which uses the Hermite functions as orthogonal windows is applied [4]. The window $h_k(n)$ will simply be the k:th Hermite function. The continuous-time Hermite functions are given by

$$h_k(t) = \frac{1}{\sqrt{\sqrt{\pi} 2^k k!}} e^{\frac{-t^2}{2}} H_k(t) \tag{2.9}$$

where

$$H_k(t) = (-1)^k e^{t^2} (\frac{d}{dt})^k e^{-t^2}. \tag{2.10}$$

2.5 Spectrogram

When a signal is non-stationary, we need to use other tools than the periodogram. The periodogram breaks down for a signal with a time dependent frequency. If we imagine a signal which has the frequency 1 Hz from t_0 to t and 2 Hz from t to t_{end}, the periodogram will show this as two peaks. One at 1 Hz and one at 2 Hz. It will not be able to say anything about the relation in time. It will look like there are two signals where there actually only is one signal, but with a varying frequency. In order to analyse the BAEP which is non-stationary we need to move over to time-frequency analysis which as

the name implies can handle a non-stationary signal i.e. a signal with a time dependent frequency [1]. Just like before with the non-parametric modelling through the periodogram, we begin with the Fourier transform.The short time Fourier transform (STFT) $X(t, f)$ of a signal $x(t)$ is defined as below,

$$X(t, f) = \int_{-\infty}^{\infty} x(t_1)h^*(t_1 - t)e^{-i2\pi f t_1}dt_1, \tag{2.11}$$

where h(t) is a window function centred at time t. In this report the Hanning window has been used. The spectrogram $S_x(t, f)$ is then defined as,

$$S_x(t, f) = |X(t, f)|^2. \tag{2.12}$$

With the spectrogram we have introduced a time domain to our frequency analysis and we can now study non-stationary signals. Figuratively the spectrogram divides the signal into short time segments through the STFT, which are assumed to be stationary. The periodogram is then computed for these stationary segments and added together. In reality, all signals are sampled and the discrete STFT is used which gives the spectrogram as,

$$\hat{S}_x(n, f) = |\sum_{n_1=0}^{N-1} x(n_1)h^*(n_1 - n)e^{-i2\pi f n_1}|^2. \tag{2.13}$$

As always in spectral analysis there is a trade off in resolution. For the spectrogram, there is a trade-off between resolution in time and in frequency. If we want a good resolution in time, we need to pick a window $h(t)$ which is narrow. This leads to a poor frequency resolution and vice versa. This is a real problem if there are several components which overlap in time and others in frequency. In this thesis the window length and resolution were decided in an ad-hoc manner from which window length was perceived to give the clearest view.

In the same manner as for the periodogram, one can sum spectrograms with a weighting factor to produce a multitaper spectrogram estimate.

$$\hat{S}_x(n, f) = \sum_{k=1}^{K} \alpha_k \hat{S}_{xk}(n, f), \tag{2.14}$$

where α_k is a weighting factor. In the report, the multitaper spectrogram is used, with weights defined in [4]. The Hermite functions are used as window functions in the same manner as in the paper cited.

2.6 Analytic Signal

When we study a real valued signal, the spectral density of the negative frequencies is a mirror image of the spectral density of the positive frequencies, $X(f) = X(-f)$. This makes the negative frequencies redundant, and the analytic signal is a convenient way to only include positive frequencies [1]. A signal is said to be analytic if $X(f) = 0$ for $f < 0$ where $X(f)$ is the Fourier transform of the signal $x(t)$. The analytic signal can be found through the Hilbert transform which is defined as

$$z(t) = F^{-1}(-i \cdot sign(f)F(x(t)) \tag{2.15}$$

where F is the Fourier transform, F^{-1} is the inverse Fourier transform and the sign function is defined as

$$sign(f) = \begin{cases} 1 & \text{if } f > 0 \\ 0 & \text{if } f = 0 \\ -1 & \text{if} f < 0. \end{cases} \tag{2.16}$$

2.7 Wigner-Ville distribution

To improve the rather poor resolution of the spectrogram, the Wigner-Ville distribution can be used. The best possible time and frequency resolution is given by the Wigner-Ville distribution [1]. The Wigner-Ville distribution is defined as below

$$W_x(t, f) = \int_{-\infty}^{\infty} z(t + \frac{\tau}{2}) z^*(t - \frac{\tau}{2}) e^{-i2\pi f \tau} d\tau. \tag{2.17}$$

The Wigner-Ville distribution will always give a better resolution than the spectrogram for a single component signal, e.g. a single sinusoidal or a single

chirp signal. A chirp signal is a sinusoid with a linearly increasing or decreasing frequency. Historically this was also one of the first distributions to be made use of.

In all it's glory however, the Wigner-Ville distribution suffers gravely from cross terms. Cross terms are terms which are located in between of all actual signal components, called auto terms. The cross terms can be twice as large as the auto components themselves. The cross terms show up no matter how far between the auto components are located in time or frequency. The cross terms will oscillate proportionally to the distance between the auto terms and the direction of the oscillations will be orthogonal to the line connecting the auto terms [1]. In case of a noisy signal, there will even be cross terms created between the noise and the auto terms. This makes interpretation of the Wigner-Ville distribution extremely difficult and the distribution is often useless for real data. In order to be able to use this distribution, a lot of work and research has been done to reduce the cross terms.

2.8 Ambiguity Domain

In order to create tools, mostly in the shape of filters called time-frequency kernels, to reduce the cross terms it is very handy to make use of the so called ambiguity domain. The ambiguity domain is related to the Wigner-Ville distribution by a 2-dimensional Fourier transform. Transforming both from the frequency domain f to the time lag domain τ, and from the time domain t to the frequency lag domain ν. Rather than expressing it in the shape of this 2-dimensional Fourier transform, the ambiguity function can be written as

$$A_z(\nu,\tau) = \int_{-\infty}^{\infty} z(t+\frac{\tau}{2})z^*(t-\frac{\tau}{2})e^{-i2\pi\nu t}dt, \tag{2.18}$$

where $z(t)$ is the analytic function and ν is the frequency lag and τ is the time lag. The ambiguity function still shows cross terms, but these show up in a different way than in the time-frequency domain. The auto terms will always end up in the center and the cross terms will end up in the periphery, away from the center. To reduce the cross terms, one can multiply the ambiguity

function with a filter, which filters out the cross terms. It is also of great importance that the filter retain the auto terms as much as possible. The filter is normally called a kernel, $\phi(\nu, \tau)$. The multiplication of the ambiguity function $A_z(\nu, \tau)$ and the ambiguity kernel, $\phi(\nu, \tau)$

$$A_z^Q(\nu, \tau) = A_z(\nu, \tau) \cdot \phi(\nu, \tau), \tag{2.19}$$

ends up like a double convolution between the Wigner-Ville distribution and the 2-dimensional Fourier transform of the ambiguity kernel

$$W_z^Q(t, f) = W_z(t, f) * *\Phi(t, f) \tag{2.20}$$

where $\Phi(t, f)$ is defined as

$$\Phi(t, f) = \int_{-\infty}^{\infty} \int_{-\infty}^{\infty} \phi(\nu, \tau) e^{-i2\pi(f\tau - \nu t)} d\tau d\nu. \tag{2.21}$$

One can note that the Wigner-Ville distribution has the ambiguity domain kernel $\phi(\nu, \tau) = 1$, which means that no reduction of neither the cross terms, nor the auto terms is made.

It should be noted that there exists four domains in time-frequency analysis. The time-frequency domain being one and the ambiguity domain being another. The two remaining domains are the Doppler domain and the time-lag domain. All domains except for the time-frequency domain are very hard to interpret and lack any intuitive explanation for most applications. This is why only the time-frequency domain has been used in this thesis.

2.9 Choi-Williams kernel

Many different kernels have been designed, especially for the reduction of cross terms. One of the most applied kernels is the Choi-Williams kernel. It is used commonly in, among other, medical applications. The Choi-Williams ambiguity kernel is defined as follows, where α is a constant

$$\phi(\nu, \tau) = e^{-\alpha(\nu\tau)^2}. \tag{2.22}$$

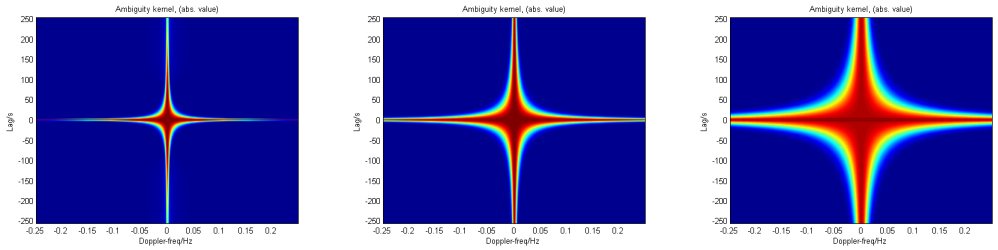

Figure 2.2: The plots show the Choi-Williams kernel in the ambiguity domain with different values of the parameter α. As the auto-terms end up in the middle of the ambiguity domain and the cross-terms outside of the middle, it is quite obvious that the Choi-Williams kernel will try to retain the auto-terms and reduce the cross-terms. From left to right $\alpha = 0.1, 1, 10$

One advantage of the Choi-Williams distribution is that it depends on the product of ν τ and hence makes for easier optimization. The constant and design parameter α decides the decay rate of the exponential function and hence how much repression of cross terms that is wanted versus how well one wants to preserve the auto terms and their resolution [2].

2.10 Doppler independent kernel

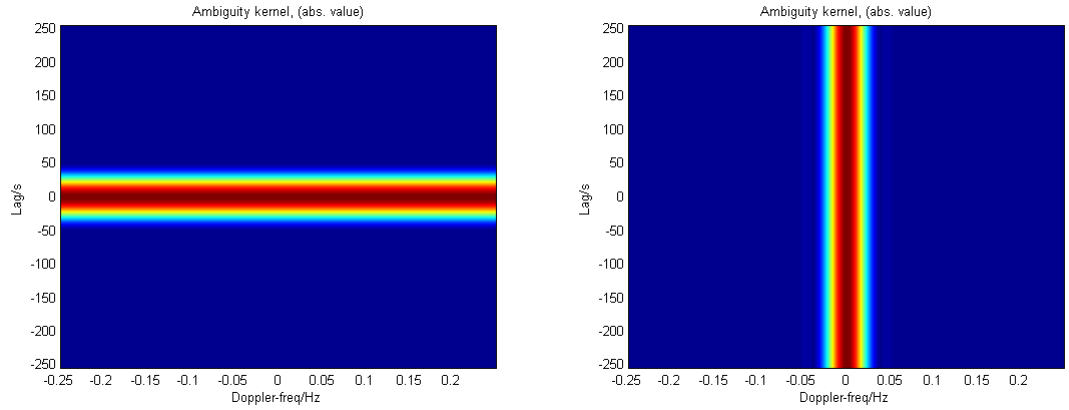

Figure 2.3: The plots show the Doppler-independent kernel and the lag-independent kernel from left to right.

Another kernel used in this thesis is the Doppler-independent kernel, which takes away all cross terms appearing from components at the same frequency, but retains the cross terms appearing from components appearing at the same time. The lag-independent kernel works in a similar manner as it removes all cross terms between terms which appear at the same time, but retains the cross terms appearing from components at the same frequency. The Doppler kernel is the only of these two kernels which performs well for the data in this thesis.

2.11 Ensemble Averaging

Ensemble averaging builds on the following assumption of a simple signal in which the potential x_i of the i:th stimulus is assumed to be additively composed of a deterministic signal component s and random noise v_i,

$$x_i = s + v_i. \tag{2.23}$$

The noise is assumed to be zero-mean, with a fixed variance σ^2 and uncorrelated over all potentials. Ensemble averaging is a straightforward way to

estimate the deterministic signal s. The estimator, which is what is used for the given data in the report is,

$$\hat{s} = \frac{1}{M}(x_1 + x_2 + ...x_M) = s + \frac{1}{M}\sum_{i=1}^{M} v_i, \tag{2.24}$$

where M is the number of potentials.
This leads to an unbiased estimator of s, with the variance

$$V[\hat{s}] = \frac{\sigma_v^2}{M}. \tag{2.25}$$

This simple model and estimator has nice properties as it is unbiased and the variance decreases with the number of potentials. Because of it's simplicity, being very intuitive and having nice properties, it is commonly used to reduce noise in the application of EP [3]. It is also the estimator used in this thesis and by SensoDetect.

2.12 The Bootstrap

Bootstrapping is a method for estimating properties of an estimator, e.g. mean and variance, by measuring those properties when sampling from a distribution approximating the real distribution. One choice of an approximating distribution is the empirical distribution. The empirical distribution derived from a sample y = $(y_1, ..., y_n)$, is the uniform distribution on the set $y_1, ..., y_n$ with distribution function

$$\hat{F}(u) = \frac{1}{n}\sum_{i=1}^{n} \mathbf{1}_{y_i \leq u} \tag{2.26}$$

where $\mathbf{1}$ is and indicator function taking the value 1 when $y_i \leq u$ and 0 otherwise.

This can be implemented by constructing a number of re-samples of the observed dataset, each of which is obtained by random sampling with replacement from the original dataset [9]. This is a straightforward way to estimate confidence intervals and variations of the peaks in the dataset. By

this method one can find out if the variation in the datasets differs and also if the peak location shows a latency shift between the awaken and the sleeping state.

Chapter 3

Models

In order to learn more about the nature of the BAEP and time-frequency analysis in general, a couple of models with varying complexity were put together. When dealing with nature in general and especially with the human brain, the most complex biological organ known to man, a model of reality is the best that one will ever get. The brain is an extraordinarily complicated system which consists of tens of billions of neurons. Each neuron has thousands of connections with other neurons. In the light of this, simplifications have to be made. The result will be a mathematical model of reality, which tries to encompass the most important properties of the real world phenomena. In such a model it is important to try to distinguish what might be an artefact with either technological origin or biological origin and what is the actual signal. Noise will also always be found in a real world situation, so it will be important for a model to be able to withstand noise. As can be seen in figure 4.1, the real data consists of a number of low frequency peaks, with small variations in time between every EP. The noise is modelled as either white or as an AR(1) process. As the real data consists of 256 samples over 15 ms, the models will consist of the same amount of samples.

3.1 Single sinusoid

The simplest model of the BAEP would be a single low frequency sinusoid. The sinusoid is windowed by a Gaussian function to make the model better and more realistic. A Gaussian windowed signal is defined as

$$x(t) = g(t - t_0)e^{-i\omega_0 t}, \tag{3.1}$$

where the unit-energy Gaussian function is

$$g(t) = \pi^{-\frac{1}{4}} e^{-\frac{1}{2}t^2}, \quad -\infty < t < \infty \tag{3.2}$$

and is often used to model a short non-stationary signal.
This model is too simple to be a meaningful model of the BAEP, but it is a starting point for evaluation and selection of which time-frequency tools to use. It is much easier to choose the correct methods and parameters when one actually knows the underlying model. The idea is then to use the knowledge gained from the simplistic model for a more complex real world situation.

The first model consisting of a single sinusoid, with a Gaussian window, centred at $t = 128$ is shown in figure 3.1.

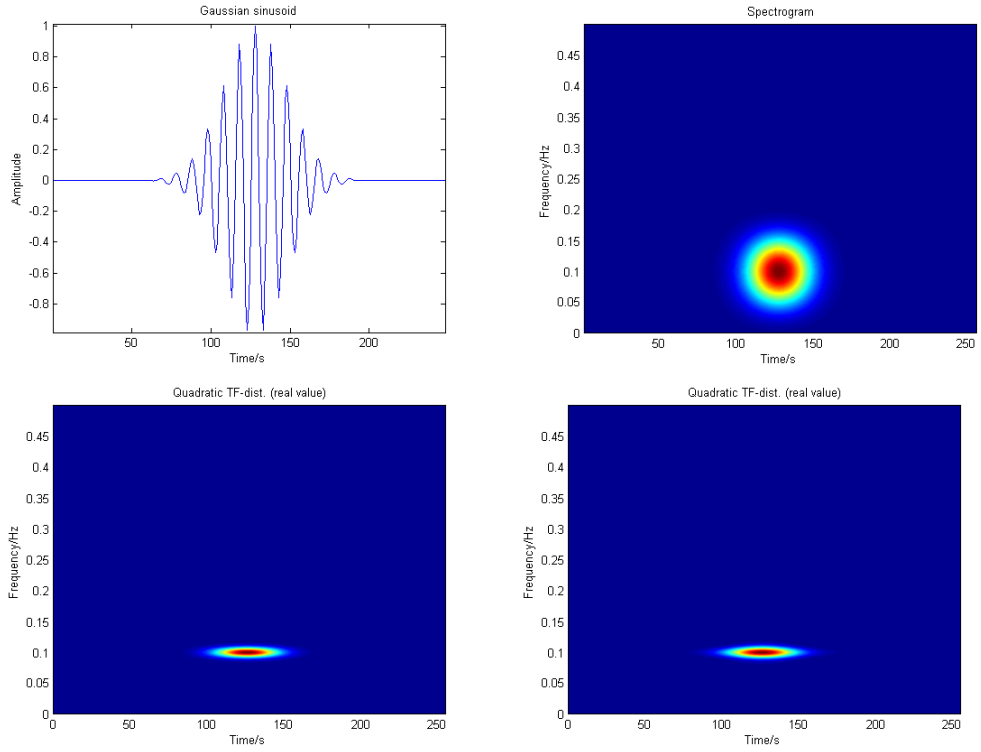

Figure 3.1: The plot in the top left corner shows a single Gaussian sinusoid, without any noise added. In the top right corner, the spectrogram with a Hanning window of length 16 is shown, and in the lower row from left to right the Wigner-Ville distribution is shown followed by the Wigner-Ville distribution with the Choi-Williams kernel $\alpha = 1$ applied.

It is a proven result that the Wigner-Ville distribution yields the best resolution for this type of single component signal. As can be seen above, the spectrogram smears the signal slightly, and the Choi-Williams kernel does little to improve or worsen the resolution, which is also an expected result as there is only one component.

The first step in making a more complex model is adding some noise, $e(t)$. This noise will be modelled as either white noise or as an AR(1) process. White noise in this case is meant as a random signal with a constant PSD, i.e. a stochastic stationary signal which contains equal power within all frequency bands. In this case it is a discrete signal which samples' are considered as a

sequence of serially uncorrelated random variables, all of which are normal distributed with zero mean and variance σ^2. The AR process is defined in it's general case in equation 2.2 with $q = 0$ and in this case the following model is used

$$x(t) + 0.5x(t-1) = e(t) \tag{3.3}$$

where e(t) is zero mean white noise with a variance σ^2.

The following model is used in figure 3.2,

$$x(t) = sin(2\pi f_0 t) + e(t) \tag{3.4}$$

where $e(t)$ is Gaussian white noise with variance $\sigma^2 = 0.25$. The signal is also windowed using equation 3.2.

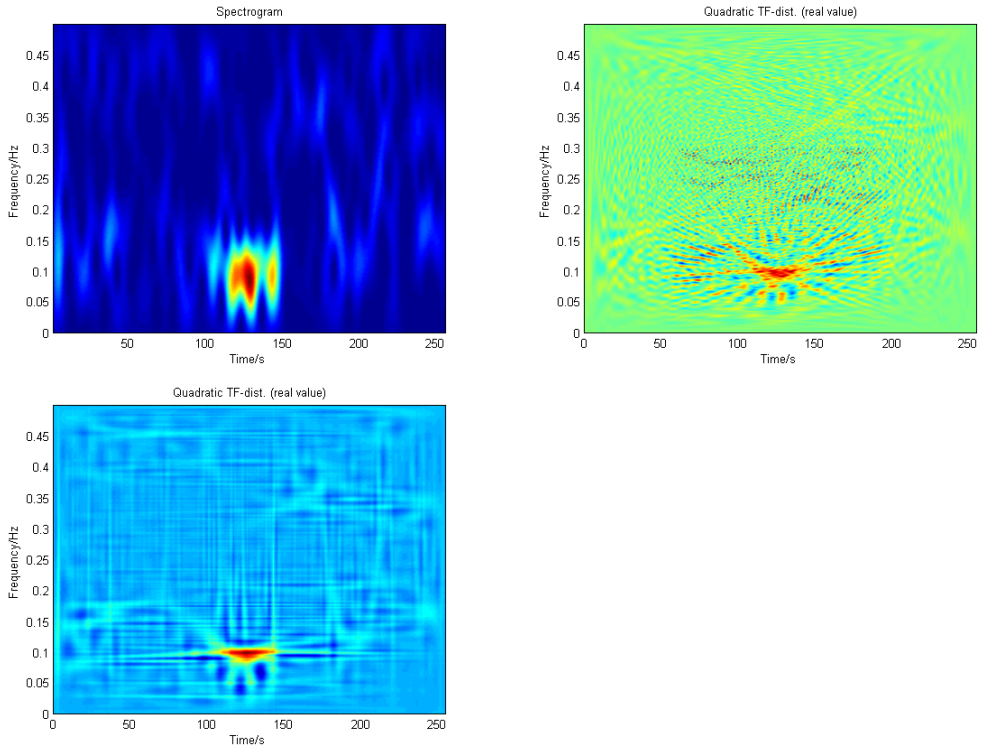

Figure 3.2: The top left plot is the spectrogram with a Hanning window of length 16. The top right plot is the Wigner-Ville distribution and the bottom left plot is the Wigner-Ville distribution with the Choi-Williams kernel $\alpha = 1$.

The signal to noise ratio is quite high in this example, and it is clear that the spectrogram loses a lot of it's resolution, but it still gives a good general idea of the signal component's location. The Wigner-Ville distribution handles this level of noise quite well, but if the noise level is increased even more, the signal component will disappear in the noise. The Choi-Williams kernel gives the best resolution for this type of white noise, the signal component is still very visible and it is more robust for a further increased noise level.

The third example of the single Gaussian sinusoid is the addition of modelling the noise as equation 3.3 with $\sigma^2 = 0.25$.

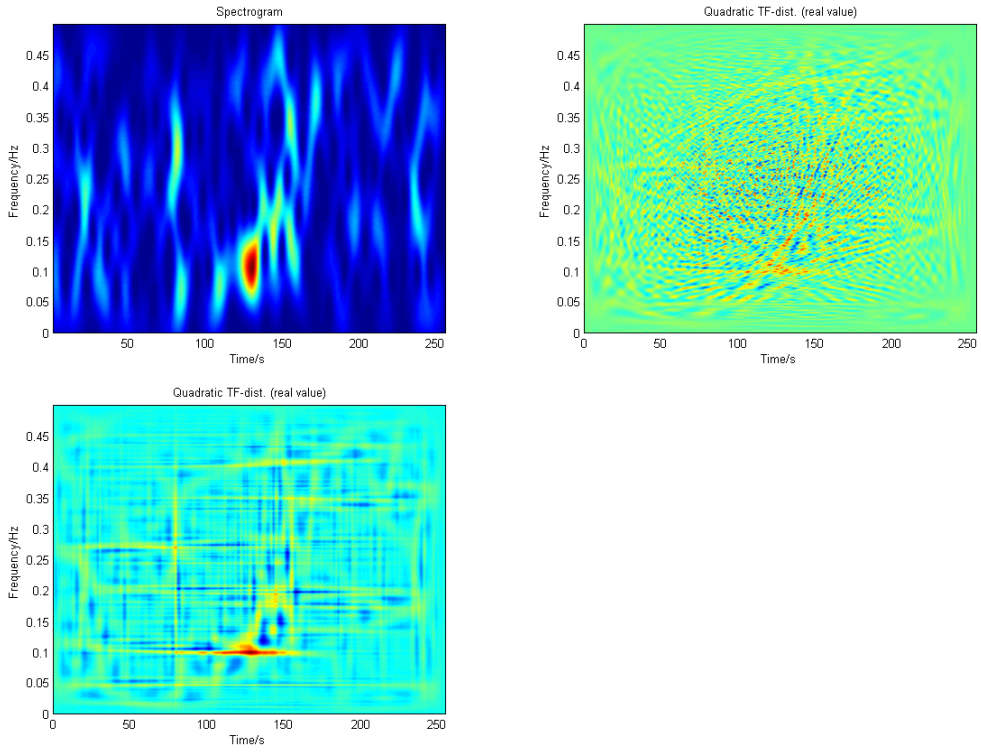

Figure 3.3: The top left plot is the spectrogram with a Hanning window of length 16. The top right plot is the Wigner-Ville distribution and the bottom left plot is the Wigner-Ville distribution with the Choi-Williams kernel $\alpha = 1$.

As can be seen above, the AR(1) noise makes the plots considerably harder to evaluate. The spectrogram still works decently, but is smeared out and components which do not belong to the Gaussian sinusoid begin to interfere. The Wigner-Ville distribution shows results which do not make sense and the Wigner-Ville distribution is not useful at all in a high noise environment like this. The Choi-Williams plot still manages to show the exact location of the signal with a good resolution and is easily the best of the three in this case.

3.2 Sum of sinusoids

Modelling a real world signal with a single time localized sinusoid is often not advanced enough. To capture all important information, one will usually

have to include more than one sinusoid. This makes time-frequency analysis very interesting as there arises cross terms in the Wigner-Ville distribution. The more advanced the model, the more obstacles have to be removed to get a clear picture of what is going on. The situation gets a lot harder to interpret when more than one signal is used as a model.

The signal model used in figure 3.4 was three complex Gaussian sinusoids. Two of them are placed at the same frequency, but separate in time. Two of the sinusoids are placed at the same time but at different frequencies. This type of model clearly shows problem with cross terms.

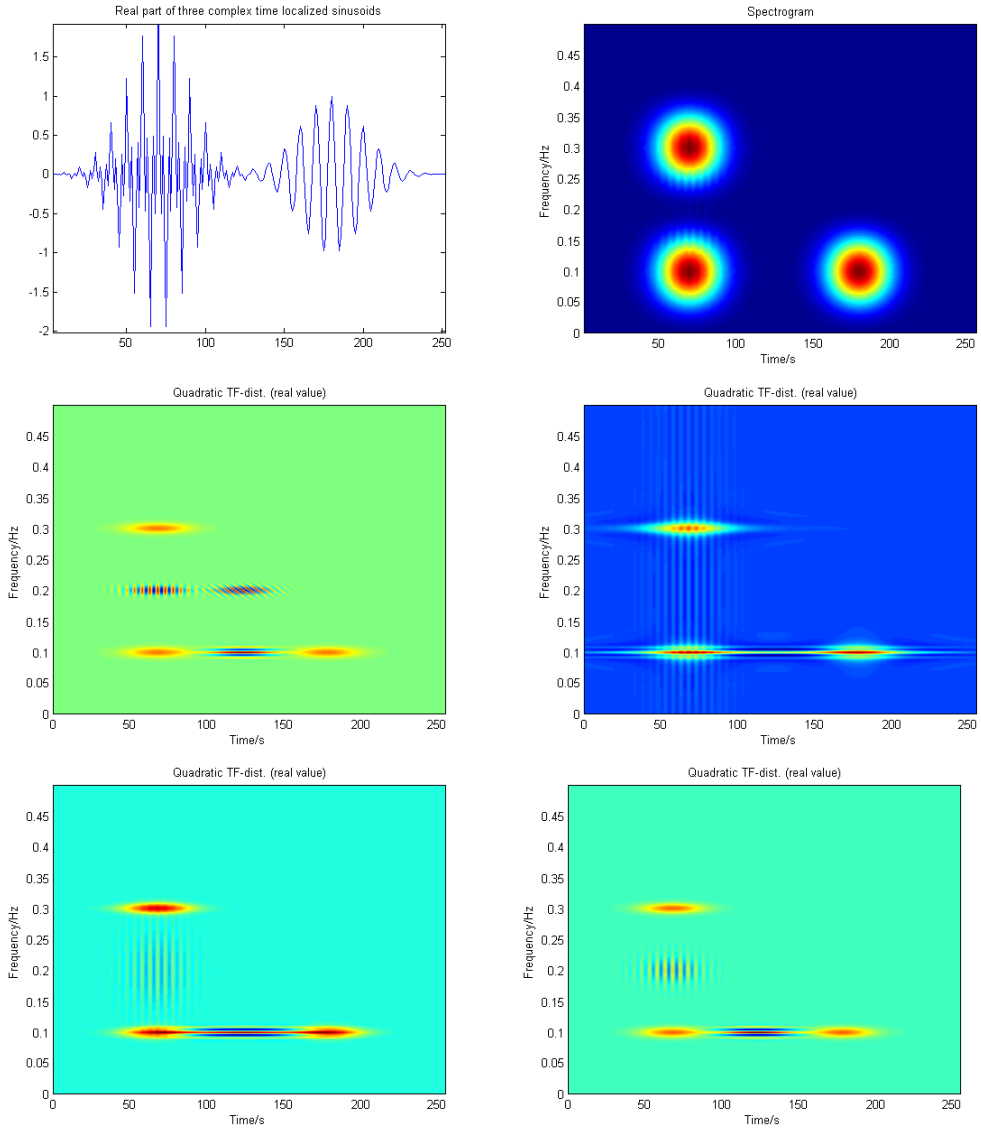

Figure 3.4: The upper left plot shows the real valued part of the signal. The upper right plot shows the spectrogram with a Hanning window of length 16. The middle left plot shows the Wigner-Ville distribution. The three following plots show the Choi-Williams distribution with three different values of the parameter, $\alpha = 0.1, 1, 10$.

It is obvious from the plot that the spectrogram does not introduce any

cross terms, which is a very nice property and helps interpretation a lot. The Wigner-Ville distribution performs very poorly, as the cross terms are as large as the auto terms themselves. The Wigner-Ville distribution is rarely useful for this type of signal, but it can be interesting to show to get an idea of how bad the cross term issues are. For the Choi-Williams distribution, the α parameter controls the decay speed of the exponential kernel. The smaller α is, the more the cross terms are suppressed. On the other hand, the smaller α is, the more the auto terms are affected. This is clearly visible if one compares the fourth plot to the sixth plot. However, a good middle of the road configuration is usually $\alpha = 1$ [2].

3.3 The Chirp

Some signals might not be possible to model with a time localized sinusoid. If the frequency of the signal for example increases or decreases as a function of time, the description has to be modified. A signal with a linearly increasing frequency, also called a chirp, is defined as

$$x(t) = sin(2\pi(f_0 t + \frac{k}{2}t^2)), \tag{3.5}$$

where

$$k = \frac{f_1 - f_0}{t_1}, \tag{3.6}$$

where f_0 is the starting frequency at $t = 0$, f_1 is the final frequency and t_1 is the ending time. As before for the sinusoidal models, the Gaussian window defined in equation 3.2 is used.

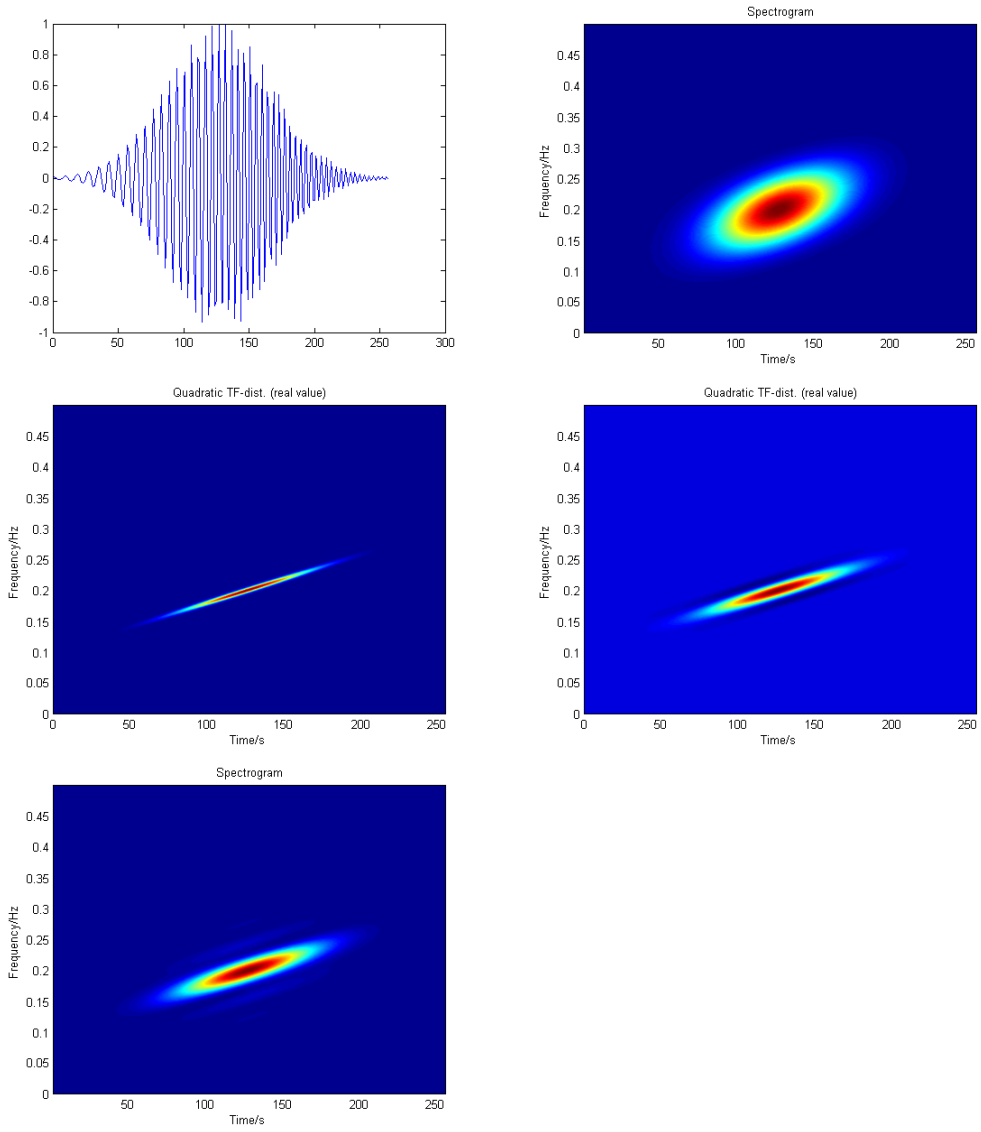

Figure 3.5: To the top left the real part of the complex windowed chirp is shown. To the top right the spectrogram with a Hanning window of length 16 is shown. The middle left plot shows the Wigner-Ville distribution. The middle right plot shows the Choi-Williams distribution with $\alpha = 1$ and the bottom left plot shows the multitaper spectrogram, using the five first Hermitian base functions.

The Wigner-Ville distribution completely nails the frequency and it is possible to show that this is the best possible resolution for this type of signal [1]. The Wigner-Ville distribution performs splendidly for this signal, but as shown earlier it handles noise and multi-component signals very poorly. The spectrogram has very poor resolution and is not very useful for this type of signal as it is hard to distinguish this picture from a simple single sinusoid without any time-frequency dependency. The Choi-Wiliams distribution gives good resolution and it is known to handle both multi-component signals and noise quite well. The multitaper spectrogram approach gives a good resolution as well.

3.4 Sum of Chirps

In order to show the boundaries for what some of these methods are able to perform, a reasonably complex signal, consisting of a sum of chirps in white noise with $\sigma^2 = 0.25$, is created.

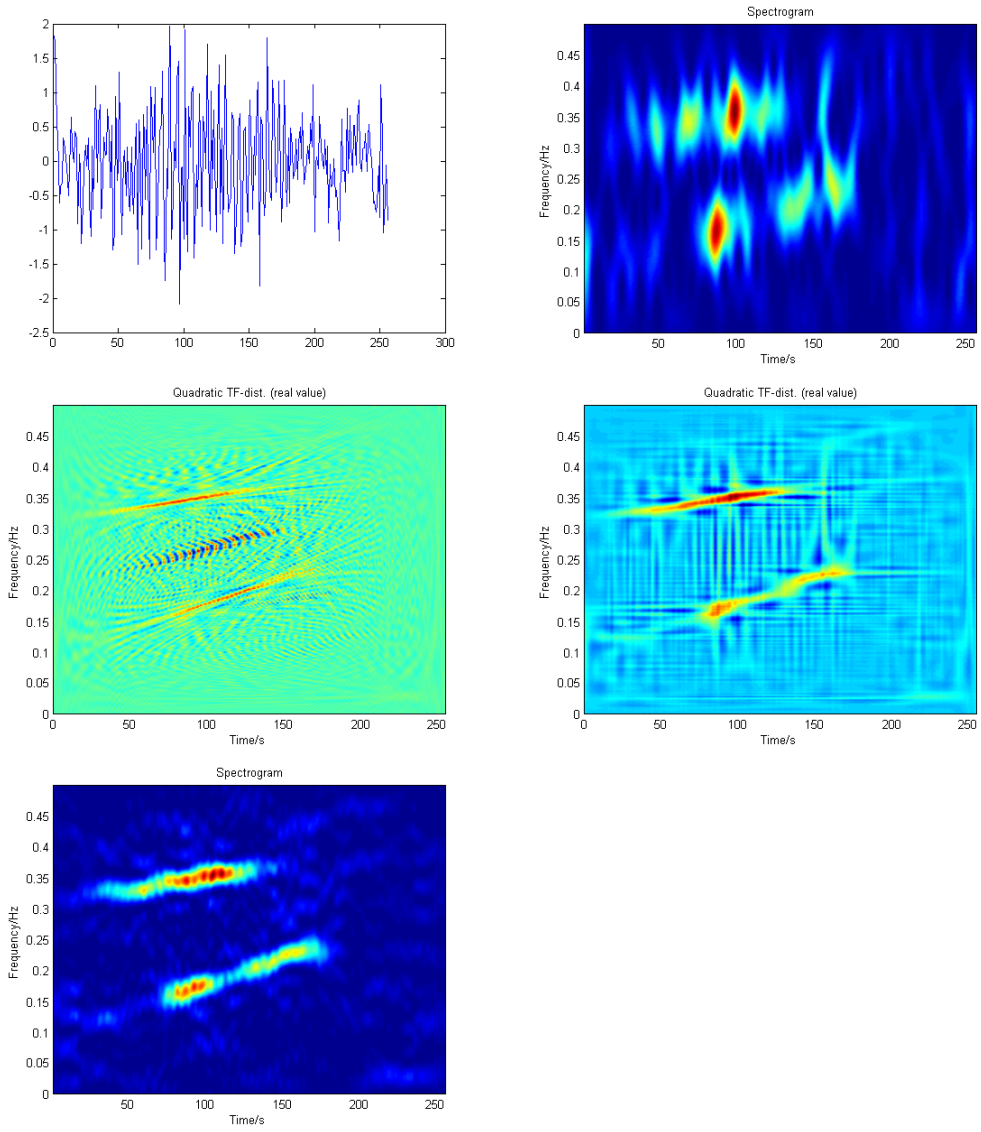

Figure 3.6: To the top left the real part of the complex windowed sum of chirps is shown. To the top right the spectrogram with a Hanning window of length 16 is shown. The middle left plot shows the Wigner-Ville distribution. The middle right plot shows the Choi-Williams distribution with $\alpha = 1$ and the bottom left plot shows the multitaper spectrogram, using the five first Hermitian base functions.

The noise level is quite high as can be seen from the first plot. The spectrogram is becoming very hard to interpret and without prior knowledge one would not be able to guess the underlying model. The same goes for the Wigner-Ville distribution with a huge cross-term and noise making it hard to see the traces of the chirps. The Choi-Williams distribution works well for this type of signal, with great cross-term suppression. However, the best method, which gives the clearest and most easily interpreted picture, is the multitaper spectrogram. It gives a picture which is free from cross terms and obviously robust even to high levels of white noise.

3.5 Stochastic Sum of Sinusoids

As a final effort to try to model the BAEP, a model consisting of a sum of six sinusoids with a stochastic amplitude and starting point was constructed. The starting points for the peaks and the amplitudes were assumed to be normal distributed. White noise was added to the signal. To be as close to the real data as possible, 90 realisations of this model were made and then the mean was taken.

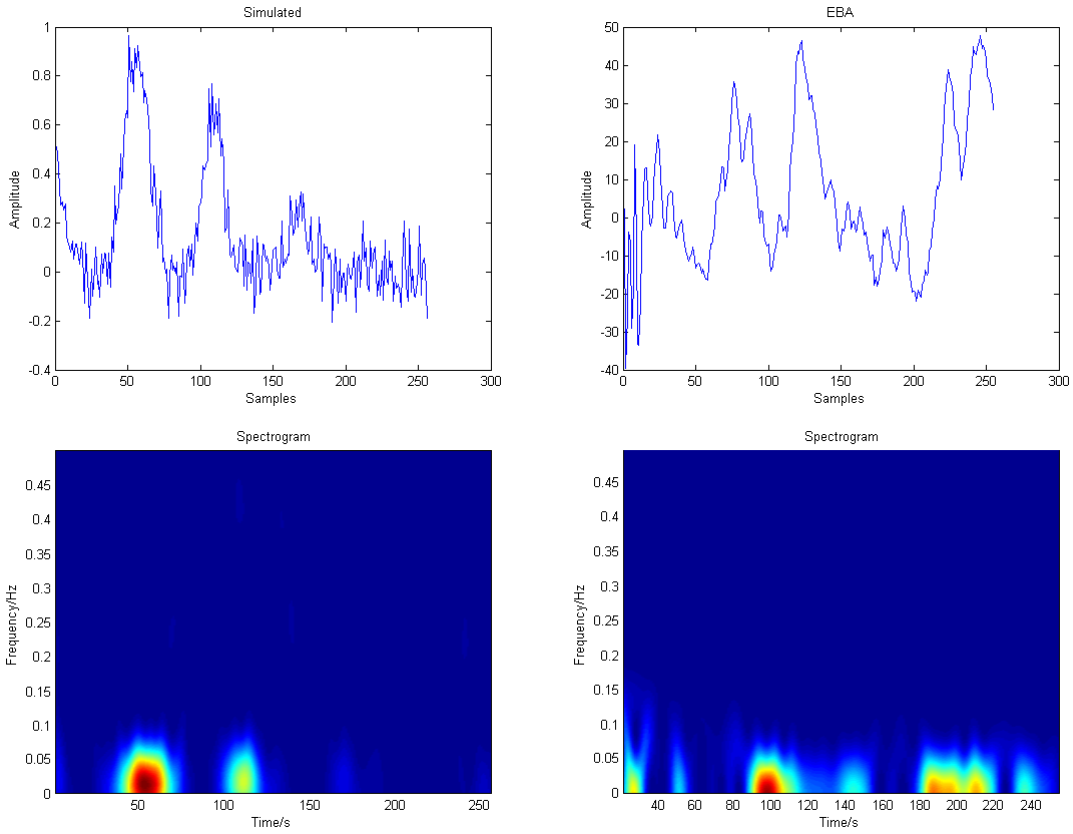

Figure 3.7: The figure shows the signal measured from the subject EB in the time domain.

As can be seen in figure 3.7 the figures are quite similar. Not similar enough to go through some sort of test for the residuals to be white, but enough to serve as a model that one may build on in the future.

Chapter 4

Results

As explained in the introduction, the data was provided by SensoDetect AB. It consisted of BAEP data from five different subjects. Four of which contained data from two measurement sessions. One session while the subject was awake, pre-operation, and one session while the subject was asleep, during operation. One dataset only contained one measurement session while the subject was awake. Each measurement session contained roughly 1300 realisations, each of them 256 samples long.

The way the data is presented is through the various spectral analysis methods explained in the theory chapter. The data will be shown as the spectrogram of sums of 30 realisations with a 50% overlap and then the mean of these spectrograms, and also as the spectrum of the mean of the entire data set. One could imagine that taking the spectrogram of each realisation and then taking the mean of all spectrograms would be an interesting approach. This is not done because of several reasons. The first being that it would require a large computational effort. Computing 1300 spectrograms per subject for each data set and each method would take a long time. The multitaper approach would require computing over 6000 spectrograms per data set. The second reason is that the data is not readily accessible in this format and would require several steps of signal processing before these computations could be done. The noise would also likely be too high to get any useful information.

From discussing with experts at SensoDetect, it is known that there is an artefact in the dataset originating from the electrical field caused by the head-

phones during the time when the click is produced and shortly afterwards. This means that the 25 first samples of the data will show something which is not the BAEP. Most of the times it precedes the first wave of the BAEP and the first 25 samples of each realisations are taken away to counter the effects of this artefact. The last 50 samples are also removed as they contain parts of what is no longer the BAEP which is studied, but rather the mid-latency EP. A rough estimate received from SensoDetect of where peaks 1-6 of the BAEP are situated in time looks as follows: Peak 1. 1.6 ms, Peak 2. 3.5 ms, Peak 3. 4.1 ms, Peak 4. 5.9 ms, Peak 5. 6.5 ms, Peak 6: 9.7 ms.

4.1 Time Domain

From simply looking at the signal in time domain one can quite easily see that there seems to be some kind of shift in latency between the red and the blue line. The later peaks in the blue signal seem to be weaker than they are for the red signal. The artefact which was mentioned above can be seen as the huge variation during the first millisecond. The later peaks for the sleeping data also seem to have vanished. The next step in investigating this signal will be to look at the signal in the frequency domain.

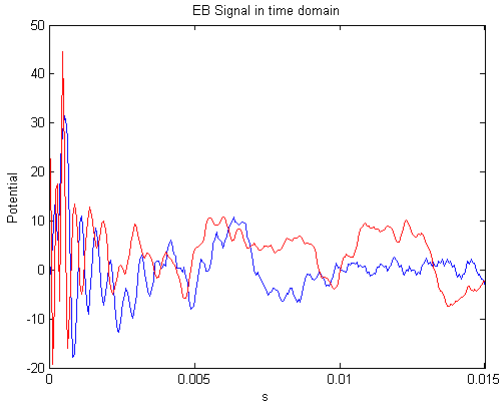

Figure 4.1: The figure shows the signal measured from the subject EB in the time domain. The red line shows the awaken data and the blue line shows the sleeping data.

4.2 Spectrum of mean

Figure 4.2 shows the spectrogram of the time mean. This means that the mean of all data has been taken in the time domain and only one spectrogram is computed. The subject labelled EB has been chosen. The awaken data is labelled EBA and the sleep data is labelled EBS. This pattern follows the rest of the report. The resulting plots for the patients other than EB have been put in the appendix.

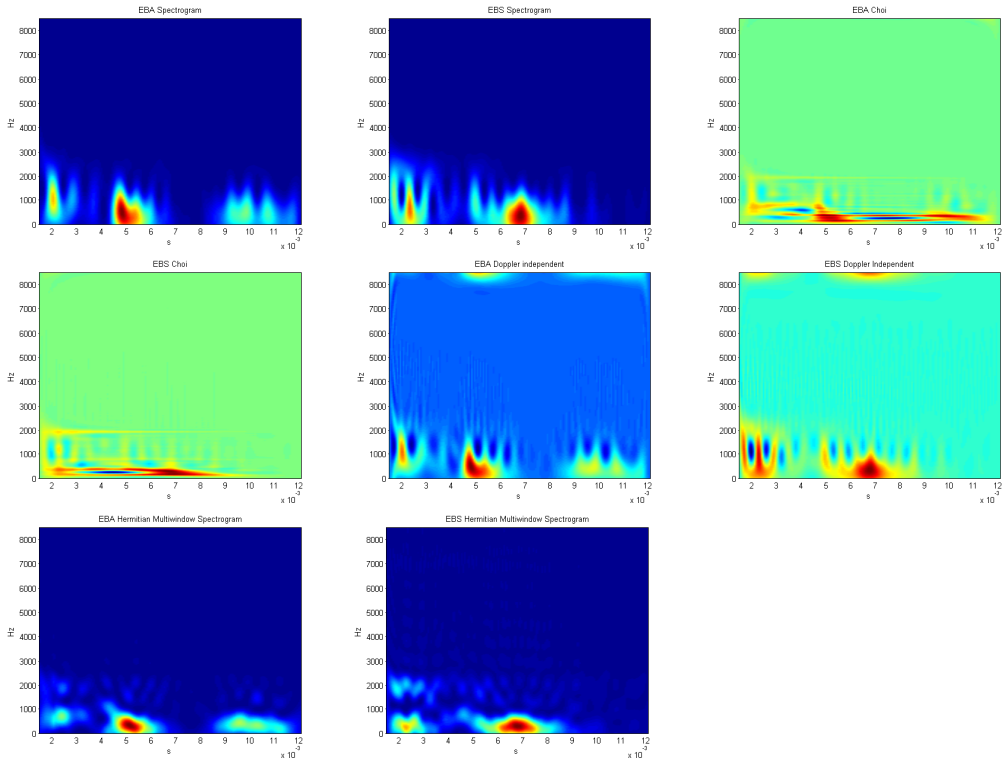

Figure 4.2: Spectrum of the mean for subject EB. The plots are shown as the awaken data first and the sleeping data second for every method. The methods used from left to right are the spectrogram with a Hanning window of length 16, the Choi-Williams distribution with $\alpha = 1$, the Doppler independent kernel with a Hanning window of length 16, and lastly the multitaper spectrogram with the 5 first Hermitian base functions.

In the ideal world, the plots would show clear red spots exactly matching the

six first waves of the EP. Some of the methods come closer to this picture than others. It is clear from the figures that the Choi-Williams distribution is significantly harder to interpret and thus concluded to be worse. The spectrogram and especially the multi-window spectrogram perform well. The multi-window spectrogram seems to give a slightly better resolution. Tese methods provide figures which are quite easy to interpret. From these two methods, one can see that there is a latency shift for the peaks from the awaken data to the sleeping data. The first peak at roughly 2 ms is moved to roughly 2.5 ms. The second and third peak usually sits together, but in the spectrogram of the awaken data one can see them slightly distinguished, the second peak at around 4.8 ms and the third at 5.2 ms. These peaks are also shifted in latency in the sleeping data and appear at around 6.8 ms. Peak 5 and 6 appear at around 9.5 ms and 10.5 ms in the awaken data. In the sleeping data, peaks 5 and 6 do not appear at all for any of the methods.

4.3 Mean of Spectrum

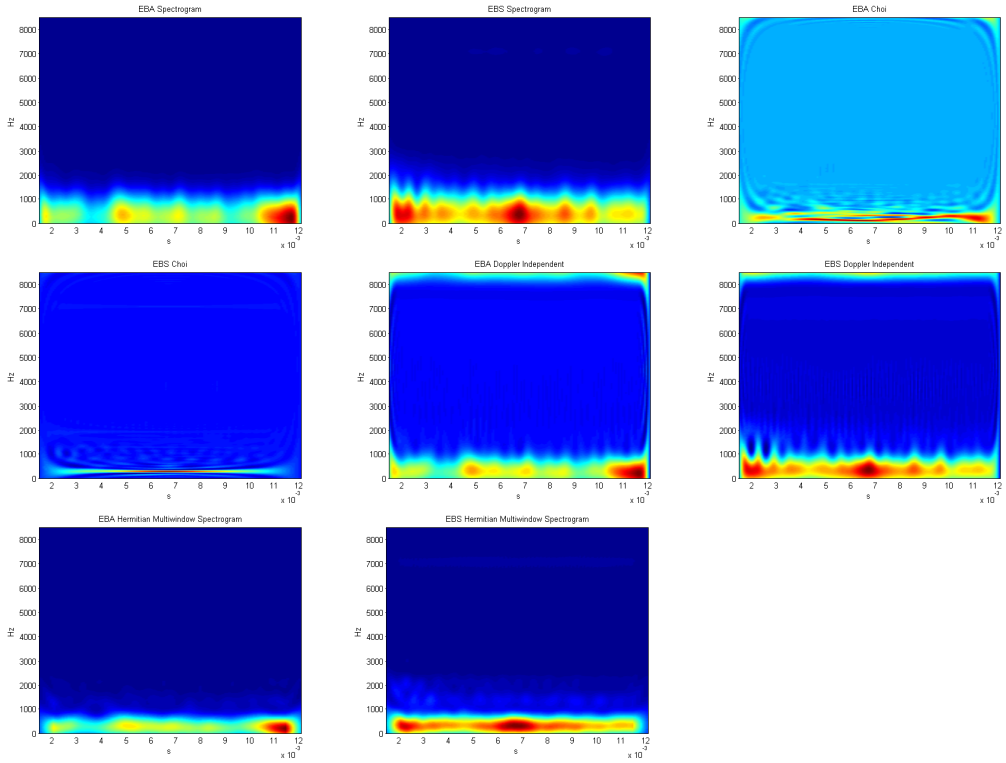

Figure 4.3: In this figure the mean of the spectrograms of the means of the 30 realisations is shown for subject EB. The plots are shown as the awaken data first and the sleeping data second for every method. The methods used from left to right are the spectrogram with a Hanning window of length 16, the Choi-Williams distribution with $\alpha = 1$, the Doppler independent kernel with a Hanning window of length 16, and lastly the multitaper spectrogram with the 5 first Hermitian base functions.

Using this kind of averaging in the spectral domain gives quite a different result. The spectrogram and the multi-window spectrogram still give the best plots, with the Doppler-independent kernel not far behind. The Choi-Williams distribution is still not giving any useful information. Instead of the peaks being quite clear in figure 4.2, there is now a lot more red and yellow spots that show up in the spectrum. This is because of the peaks varying

in latency between each 30 mean. The peaks have a natural variation and with this averaging the peaks varying enough to put them out of their center value show up. The later peaks that where not visible in figure 4.2 for peaks 5 and 6 are now visible. There seems to be a shift in latency for peak one from 2 ms to 2.5 ms, for peak 2 from 5 ms to 6.5 ms and peak 4 from 7 to 8.5 ms. Peak 5 and 6 seem to have been shifted from around 8.5 ms to 10.5 ms. However, these observation are not really reliable, as it is quite difficult to say anything about which peak is which. This issue is a lot bigger than for the spectrum of the mean. The bottom line is now completely yellow with a lot of red spots appearing. With some good will and imagination, one could place the peaks wherever one wants.

4.4 Bootstrap

As a final attempt to take a more mathematical approach to the issue of finding a latency shift in the data, a bootstrap method was pursued. The 90 30 means were used. For each of these means the highest value for the peaks was taken. As peaks 2 and 3, and 4 and 5 are quite close together and hard to distinguish, they were assumed to be together. This means that the highest value in the region were peak 1 is usually found, which is 2-3 ms was taken as the location for peak 1. The same follows for the rest of the peaks, with peak 2 and 3 assumed to be at 3.2-5.2 ms and peak 4 and 5 assumed to be at 5.3-8.5 ms and lastly peak 6 is assumed to be at 8.5 ms to 12 ms. The values for these peaks are then taken, with replacement, for randomly picked realisations chosen out of the 90 30 means.

As a start 1000 realisations were chosen out of the 90 30 means. From these realisations an average and confidence bounds were computed, assuming that the peak locations are independent. The table below shows the etimates of the mean peak location and their 95% confidence bounds. In the first two tables the computations are done for subject EB and in the third table for the stochastic sinusoid model. The first and third table uses time domain data and the second uses spectral domain data.

	Awake	Sleeping
peak 1	43.24±0.53	41.59±0.48
peak 2-3	75.51 ±0.58	75.49±0.64
peak 4-5	115.60 ± 0.89	117.47 ±0.91
peak 6	181.89± 1.20	174.16±1.24

	Awake	Sleeping
peak 1	42.52±0.53	42.86±0.55
peak 2-3	74.76 ±0.59	75.46±0.64
peak 4-5	119.63± 0.84	114.58 ±0.94
peak 6	182.37± 1.12	173.96±1.17

	Model data
peak 1	47.23±0.53
peak 2-3	70.42 ±0.61
peak 4-5	104.72± 0.57
peak 6	163.10±0.55

Unfortunately this attempt to bootstrap the peak latencies does not fall out well. The expected latency shift is not there and it seems like the algorithm misses peak 1 completely. However, one thing that was predicted is shown. The variation for the latest peak is more than twice as large as the variation for the first peaks. This means that peak 6 will vary much in time and may disappear when taking an average.

For the modelled data the bootstrap finds peak 2-3, 4-5 and 6 well, but misses peak 1 completely. This means that the peak finding algorithm has to be refined, at least for peak 1. The variation is in the same region for the first peaks, but for peak 6 the modelled variation is only half the variation from the real data. This could be used to further improve the stochastic sinusoid model.

Chapter 5

Discussion

In the model part of the report I conclude that the Wigner-Ville distribution performs very well for a single component signal without noise. In a high noise environment the Choi-Williams distribution performs the best. An α of 1 is usually the best parameter choice. The models that contain sums of signals are more interesting as they show the problem with cross terms. For these simple models, the Choi-Williams distribution is very good and the Wigner-Ville distribution almost useless. For the chirp signals, the multi-window spectrogram shines. It is the best performing method for the sum of chirps model. The model part could be continued by chirps with a quadratic, exponential or even sinusoidal dependency on the frequency. However, sufficiently many real world signals can be described by the models up to this point. Should a real world phenomena occur with the need of a more complex model, then I think that, thanks to the section above, I have enough experience with the simpler models to tackle them.

The stochastic sum model is very interesting as it comes close to the real signal model. This model could be made even better with more refined parameter values. I conclude that it is a good starting point for someone who might to investigate the model further.

It has been quite hard to quantify any results from the plots under the result chapter. It is clear that the Choi-Williams distribution does not work out at all, and that the multi-window spectrogram gives the clearest view. The hypothesis of the latency shift between the awaken and sleeping data set seems to be valid for some of the patients and some of the peaks. The earlier peaks

seem to be shifted in latency while the later peaks seem to disappear for the sleeping data. Looking at the mean of the spectrum plots one can see that there is still activity in the later part of the sleeping data, but it cancels out in the spectrum of the mean. It is possible that the later peaks have a lower amplitude and are more out of sync and therefore cancelling each other out in the spectrum of the mean.

In the bootstrap section there are some issues which may have given a strange result. The first is that in order to pick out each of the peaks an assumption had to be made for which region each peak will be found in. If these regions overlap there is a real problem knowing which peak is which. For peaks two and three and four and five, they will very often overlap. The thing is then that only one out of the pairs of the peaks will be found, yielding some strange results. The method for finding these peaks could be refined and in that case the algorithm will yield a better result. There is also some doubt in using the assumption of the peak latencies being independent. There is some vague pattern that shows for some peaks, but this is overlooked and they are assumed to be independent.

Some points where I have struggled more than others should be noted. The area of BAEP is quite hard to work with as it is not a very frequent research area. The knowledge is not very great of exactly what is going on in the BAEP so it has been hard knowing what to look for in the data. I also think that I should have kept myself to one set of data and making the algorithms work better for that set before extending into a larger data set. The BAEP data itself is also extremely noisy and in general quite hard to interpret.

I think that the limitations of not going into detail with the signal processing of SensoDetect was a good idea. It would have been a thesis on it's own to understand completely what they do and to improve it. It would require a lot more input from SensoDetect which was not available. I am also not sure that I would have been able to improve it as they do get quite clear results. It might simply be that this type of data is very hard to work with and that the BAEP differs from patient to patient.

To continue this work I would continue with the stochastic model. I would refine it and use center values and standard deviation values from the real data. I would not continue with analysing the real data as it has proved

quite challenging. I would have liked to take a more mathematical approach to analysing the data and to be able to quantify for example a latency shift, but it has proven to be quite tricky.

Bibliography

[1] M. Sandsten *Time-Frequency Analysis of Non-Stationary Processes - An Introduction* Lund: Centre for Mathematical Sciences, 2013.

[2] S. Qian and D. Chen, *Joint Time-Frequency Analysis - Methods and Applications*. Prentice Hall 1996.

[3] L. Sörnmo and P. Laguna, *Bioelectrical Signal Processing in Cardiac and Neurological Applications*. Amsterdam: Elsevier (Academic Press), 2005.

[4] F. Cakrak and P. Loughlin, "Multiwindow Time-Varying Spectrum with Instantaneous Bandwidth and Frequency Constraints" *IEEE Transactions on Signal Processing* vol 49, No 8, 2001.

[5] M. Hansson, T. Gänsler and G. Salomonsson, "A System for Tracking Changes in the Mid-Latency Evoked Potential During Anesthesia" *IEEE Transactions on Biomedical Engineering* vol 45, No 3, 1998.

[6] J. Källstrand, S. Nehlstedt et al, "Lateral asymmetry and reduced forward masking effect in early brainstem auditory evoked responses in schizophrenia" *A Psychiatry Res.* vol 196, No 2-3 2012.

[7] G. Lindgren, H. Rootzén and M. Sandsten, *Stationary Stochastic Processes*. Lund: Centre for Mathematical Sciences, 2009.

[8] P. Stoica and R. Moses, *Introduction to Spectral Analysis* Prentice Hall, 1997.

[9] M. Sköld, *Computer Intensive Statistical Methods* 2006.

Chapter 6

Appendix

In the appendix the result plots are shown for the rest of the subjects.

6.1 Time domain

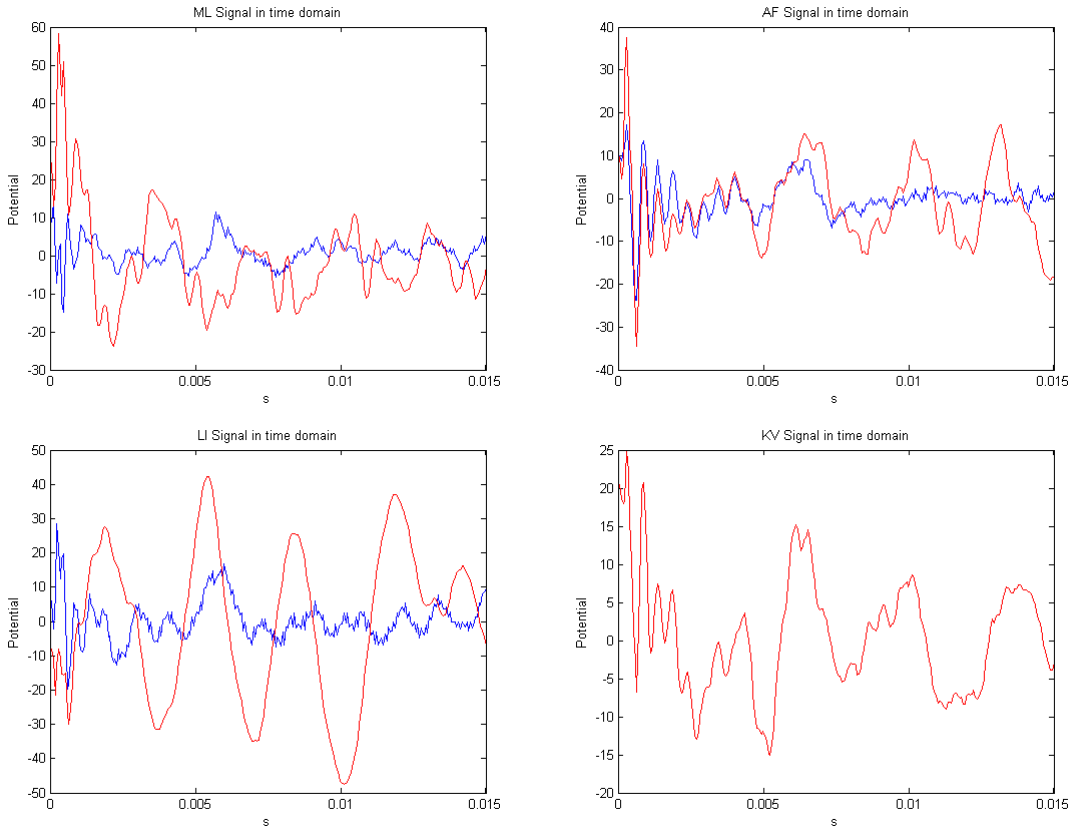

Figure 6.1: The figure shows the signal measured from the subjects ML,AF,LI and KV in the time domain. The red line shows the awaken data and the blue line shows the sleeping data.

From figure 6.1 we can conclude that the awaken measurement for LI seems to be very strange. It is likely that something has gone wrong either while measuring or in the pre-processing. For subjects ML and AF the pattern with a slight latency shift from awaken to sleeping seems to be present. The later peaks for the sleeping data seem to have disappeared completely. For subject KV only the awaken data is available, but there seem to be six clear peaks in that data.

6.2 Spectrum of Mean

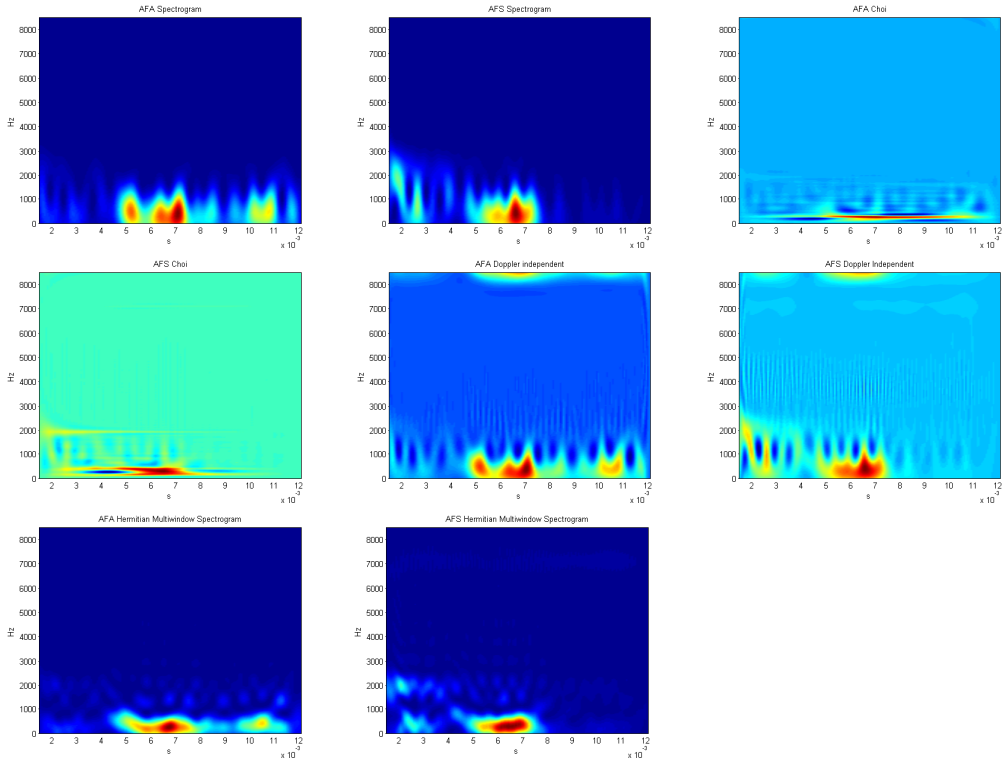

Figure 6.2: Spectrum of the mean for subject AF. The plots are shown as the awaken data first and the sleeping data second for every method. The methods used from left to right are the spectrogram with a Hanning window of length 16, the Choi-Williams distribution with $\alpha = 1$, the Doppler independent kernel with a Hanning window of length 16, and lastly the multitaper spectrogram with the 5 first Hermitian base functions.

There seems to have been some sort of shift from awaken to sleeping data, but it is hard to say as there is only one clear peak in the sleeping spectrogram. For the awaken data one can find five peaks with some imagination, but in the sleeping data only 3 seem to be visible.

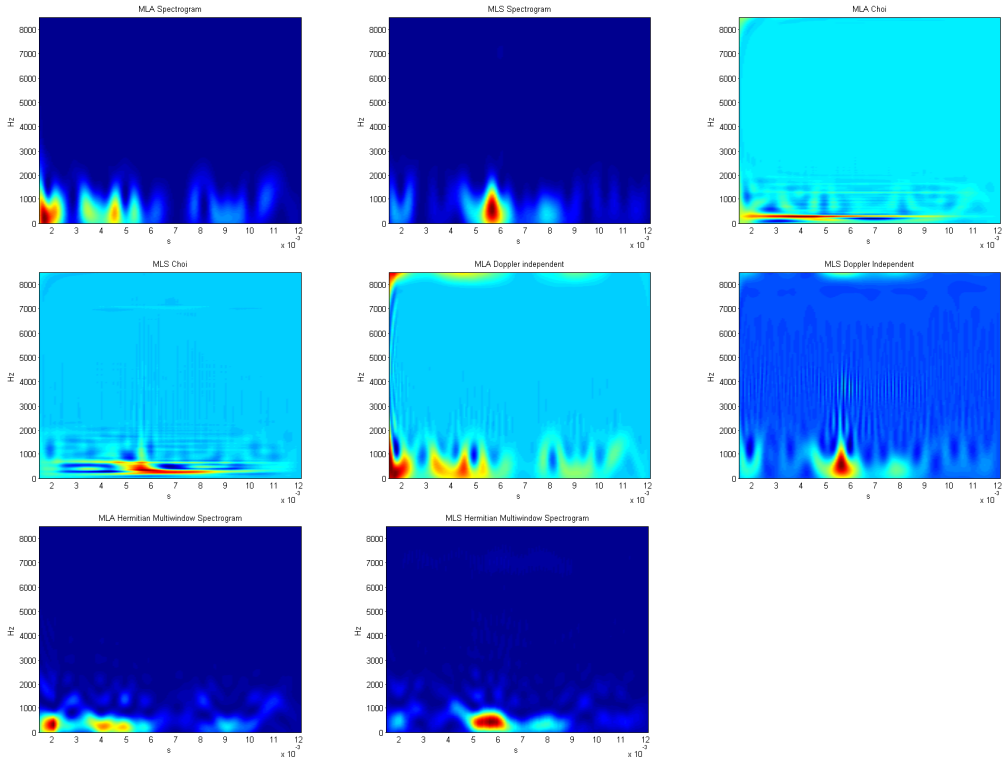

Figure 6.3: Spectrum of the mean for subject ML. The plots are shown as the awaken data first and the sleeping data second for every method. The methods used from left to right are the spectrogram with a Hanning window of length 16, the Choi-Williams distribution with $\alpha = 1$, the Doppler independent kernel with a Hanning window of length 16, and lastly the multitaper spectrogram with the 5 first Hermitian base functions.

For this subject there are four visible peaks in the awaken data. The same goes for the sleeping data. Peak 1 is visible in both datasets at 2 ms. It is likely that the peaks at 4 and 5 ms in the awaken data has moved to around 5.5 ms in the awaken data. It is not likely that the peak at 9 ms has moved backwards to 8 ms. That leads one to think that the peak visible at 8 ms in the sleeping data is a peak which is not visible in the awaken data.

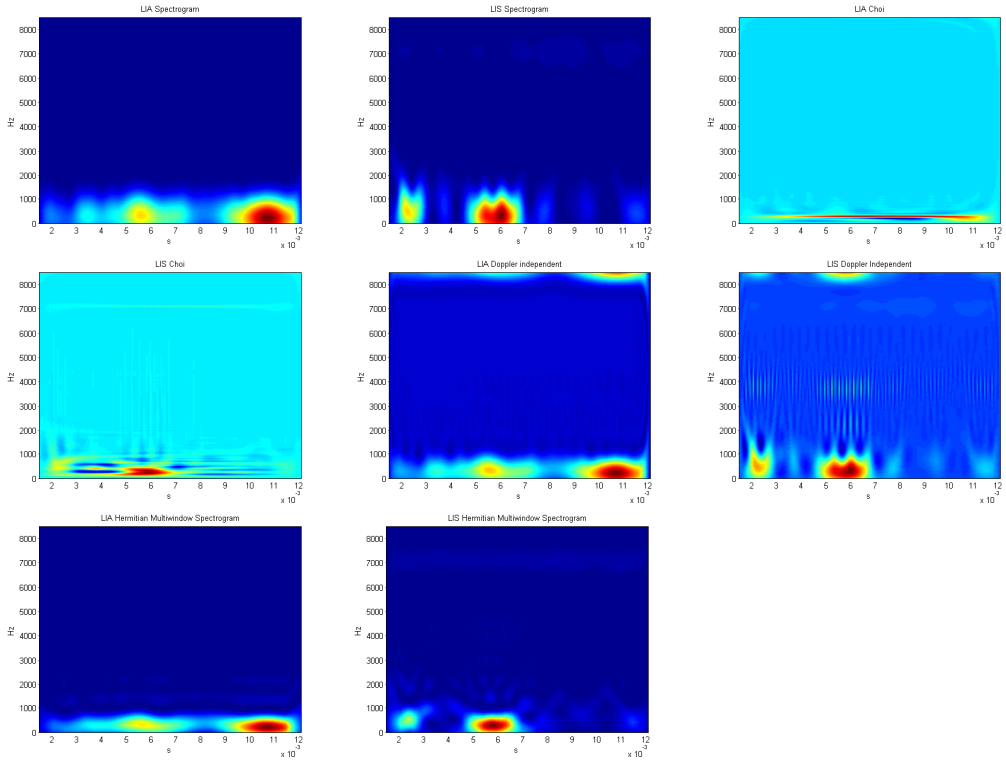

Figure 6.4: Spectrum of the mean for subject LI. The plots are shown as the awaken data first and the sleeping data second for every method. The methods used from left to right are the spectrogram with a Hanning window of length 16, the Choi-Williams distribution with $\alpha = 1$, the Doppler independent kernel with a Hanning window of length 16, and lastly the multitaper spectrogram with the 5 first Hermitian base functions.

For this subject, the peaks in the awaken data seem quite clear, but it was concluded to be a very strange measurement from looking at the time domain. There seems like there are only 3 peaks in the sleeping data.

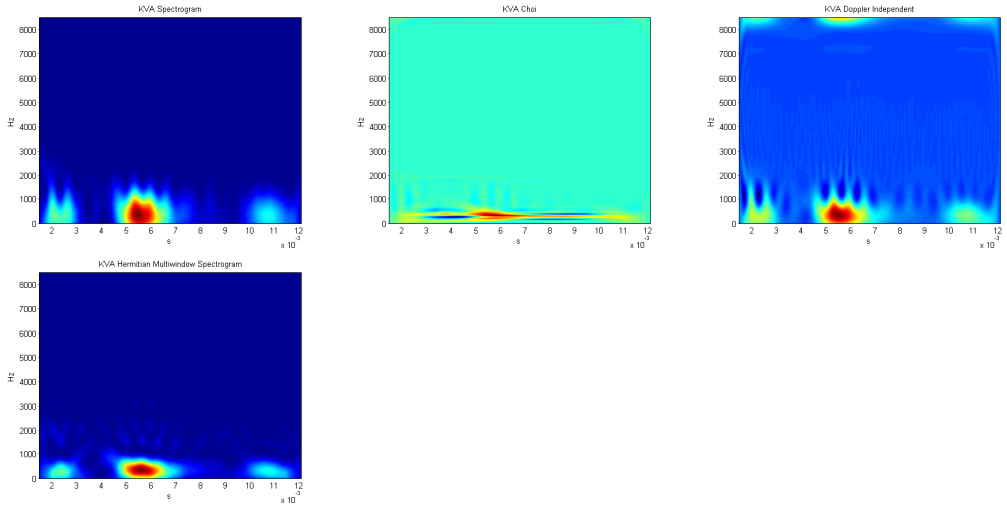

Figure 6.5: Spectrum of the mean for subject KV. Only awaken data was available. The methods used from left to right are the spectrogram with a Hanning window of length 16, the Choi-Williams distribution with $\alpha = 1$, the Doppler independent kernel with a Hanning window of length 16, and lastly the multitaper spectrogram with the 5 first Hermitian base functions.

It is quite hard to say how many peaks there are from the spectrograms, but four peaks seem to be visible.

6.3 Mean of Spectrum

For all of the subjects these plots are hard to interpret. The awaken data shows as a long red line, which might point to a big variation in the awaken dataset. For the sleeping data all peaks show up, but it is quite hard to make any statements about where the peaks begin and where they end.

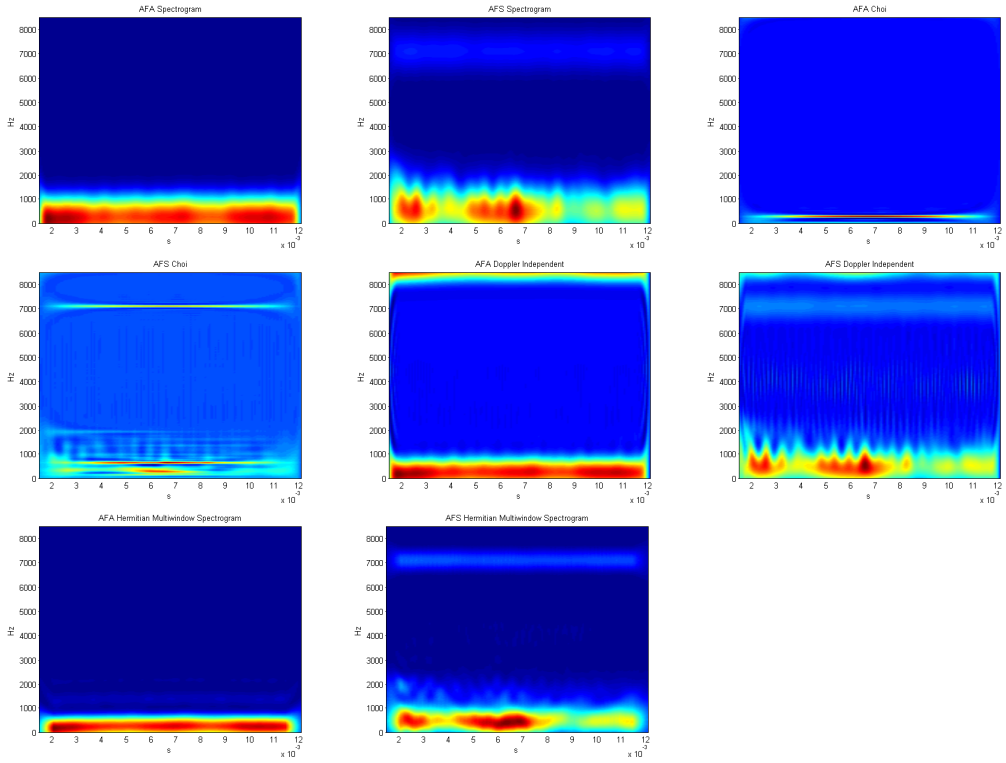

Figure 6.6: In this figure the mean of the spectrograms of the means of the 30 realisations is shown for subject AF. The plots are shown as the awaken data first and the sleeping data second for every method. The methods used from left to right are the spectrogram with a Hanning window of length 16, the Choi-Williams distribution with $\alpha = 1$, the Doppler independent kernel with a Hanning window of length 16, and lastly the multitaper spectrogram with the 5 first Hermitian base functions.

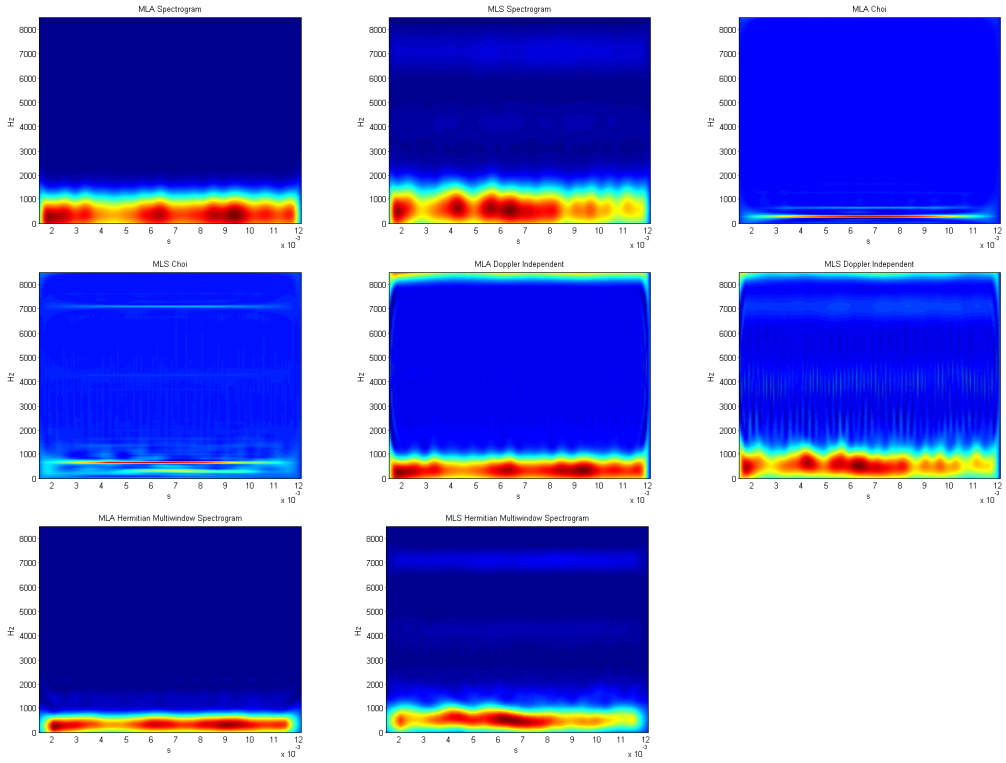

Figure 6.7: In this figure the mean of the spectrograms of the means of the 30 realisations is shown for subject ML. The plots are shown as the awaken data first and the sleeping data second for every method. The methods used from left to right are the spectrogram with a Hanning window of length 16, the Choi-Williams distribution with $\alpha = 1$, the Doppler independent kernel with a Hanning window of length 16, and lastly the multitaper spectrogram with the 5 first Hermitian base functions.

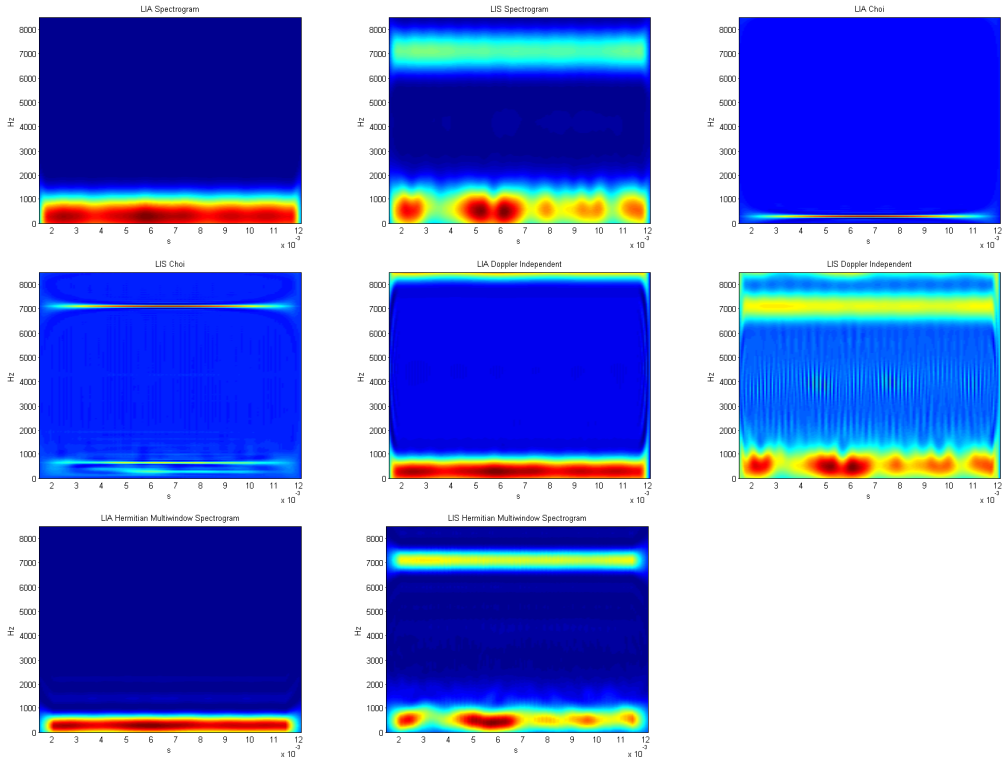

Figure 6.8: In this figure the mean of the spectrograms of the means of the 30 realisations is shown for subject LI. The plots are shown as the awaken data first and the sleeping data second for every method. The methods used from left to right are the spectrogram with a Hanning window of length 16, the Choi-Williams distribution with $\alpha = 1$, the Doppler independent kernel with a Hanning window of length 16, and lastly the multitaper spectrogram with the 5 first Hermitian base functions.

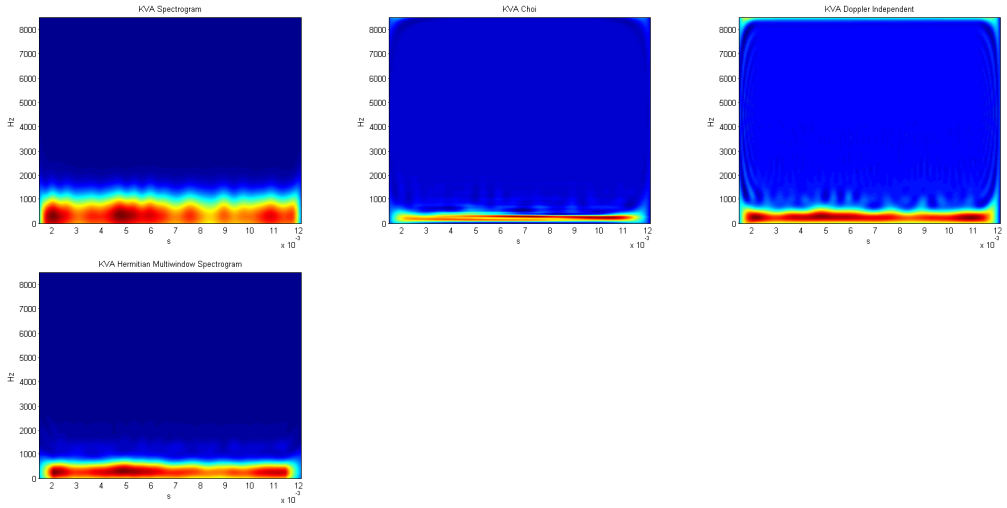

Figure 6.9: In this figure the mean of the spectrograms of the means of the 30 realisations is shown for subject KV. Only awaken data was available. The methods used from left to right are the spectrogram with a Hanning window of length 16, the Choi-Williams distribution with $\alpha = 1$, the Doppler independent kernel with a Hanning window of length 16, and lastly the multitaper spectrogram with the 5 first Hermitian base functions.

Populärvetenskaplig sammanfattning

Inledning

Detta arbete har handlat om att analysera hjärnstamssvaret från Auditory Evoked Potentials (AEP). Med evoked potential menas en hjärnsignal som triggas av ett sensoriskt intryck och med ett AEP menas att detta sensoriska intryck är ett kort ljud. I detta fall ett kort klickljud. Hjärnstammen är den allra primitivaste delen av hjärnan och basala intryck, som att registrera att vi har hört ett ljud, sker här. Det visar sig att det finns intressanta samband hos hjärnstamssvaret och psykiska sjukdomar såsom schizofreni och ADHD. Ett lundabaserat företag som heter SensoDetect AB har specialiserat sig i denna typ av diagnostik. De lyckas diagnostisera dessa sjukdomar vid 80% av fallen och deras objektiva diagnostiseringsmetod är tänkt som ett komplement till psykiatriska undersökningar som vanligen görs för att fastställa en diagnos. Det som är bra med denna metod är att man kan få information om hur nervsystemet fungerar utan att behöva göra ett enda snitt på patienten. Patienten tar på sig ett par hörlurar och elektroder fästs på skallen. Sedan spelas ungefär 1500 klickljud upp och signalen mäts automatiskt och patienten behöver inte göra någonting. Hjärnstamssvaret är en extremt brusig signal och för att få fram en signal som går att tolka så måste man ta ett medelvärde över många signaler. Detta är anledning till att patienten får höra 1500 klickljud. Detta är ett relativt outvecklat forskningsområde. Signalen uppvisar ett beteende där frekvensinnehållet ändras med tiden. Detta gör det till en ganska svåranalyserad signal. Med hjälp av något som kallas tidsfrekvensanalys kan man däremot analysera signaler som har ett frekvensinnehåll som förändras över tiden.

Målet med själva arbetet har bestått av två delar. Den ena delen har varit att komma på och undersöka olika modeller för hjärnstamssvaret. Den andra delen av arbetet har bestått i att analysera data från riktiga patienter som har erhållits ifrån SensoDetect och undersöka om det finns någon information man kan få fram genom tidsfrekvensanalys.

Modeller och Resultat

En hel del olika modeller av varierande komplexitet provades. Dessutom användes en hel del olika tidsfrekvensmetoder för att analysera modellen. Den bästa modellen bestod av en summa av enkla signaler med en slumpmässig variation i startvärde och amplitud. Modellsignalen kan ses i figur 6.10 där den jämförs med riktiga data.

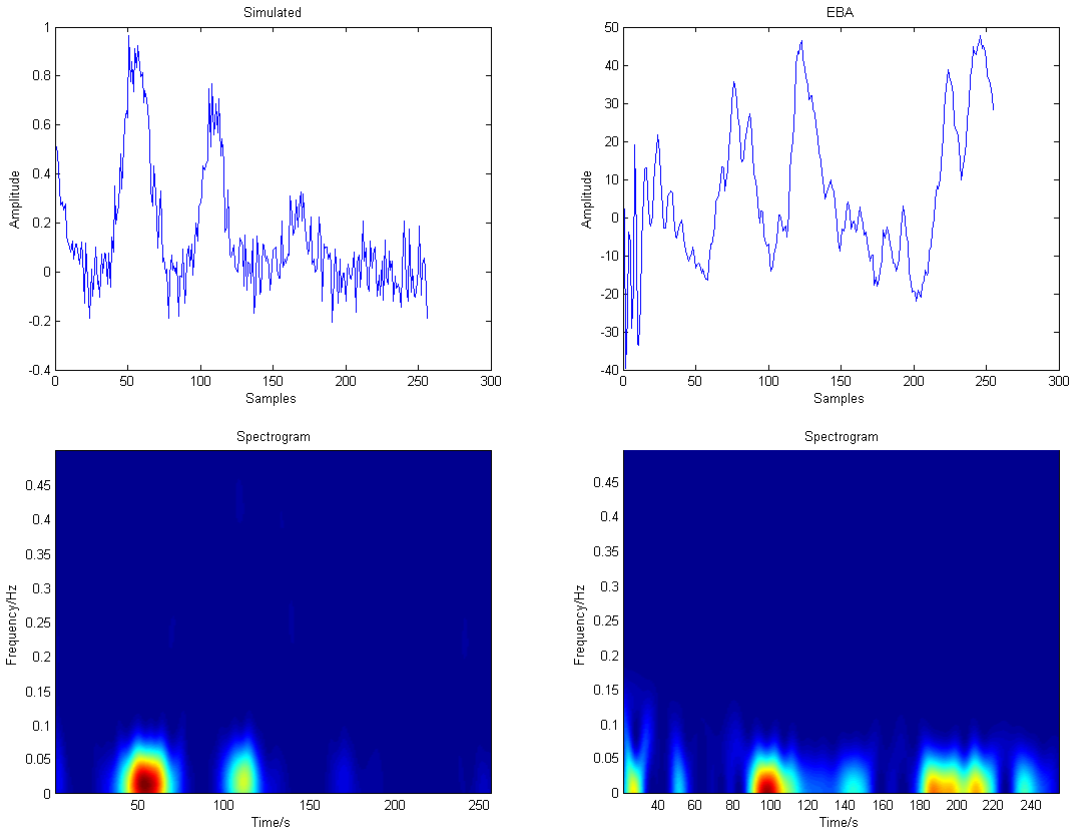

Figure 6.10: Från vänster till höger på den översta raden visas den modellerade signalen följt av signalen från patient EB. Bottenraden visar spectrogrammet av signalen ovanför. Spectrogrammet är kort sagt ett stt att visa signalen i frekvensdomänen och tidsdomänen samtidigt.

Den riktiga datan bestod av mätningar först när patienten var vid vaket tillstånd och sedan mätningar när patienten var sövd under operation. En jämförelse av signalen för patienterna kan ses nedan i figur 6.11.

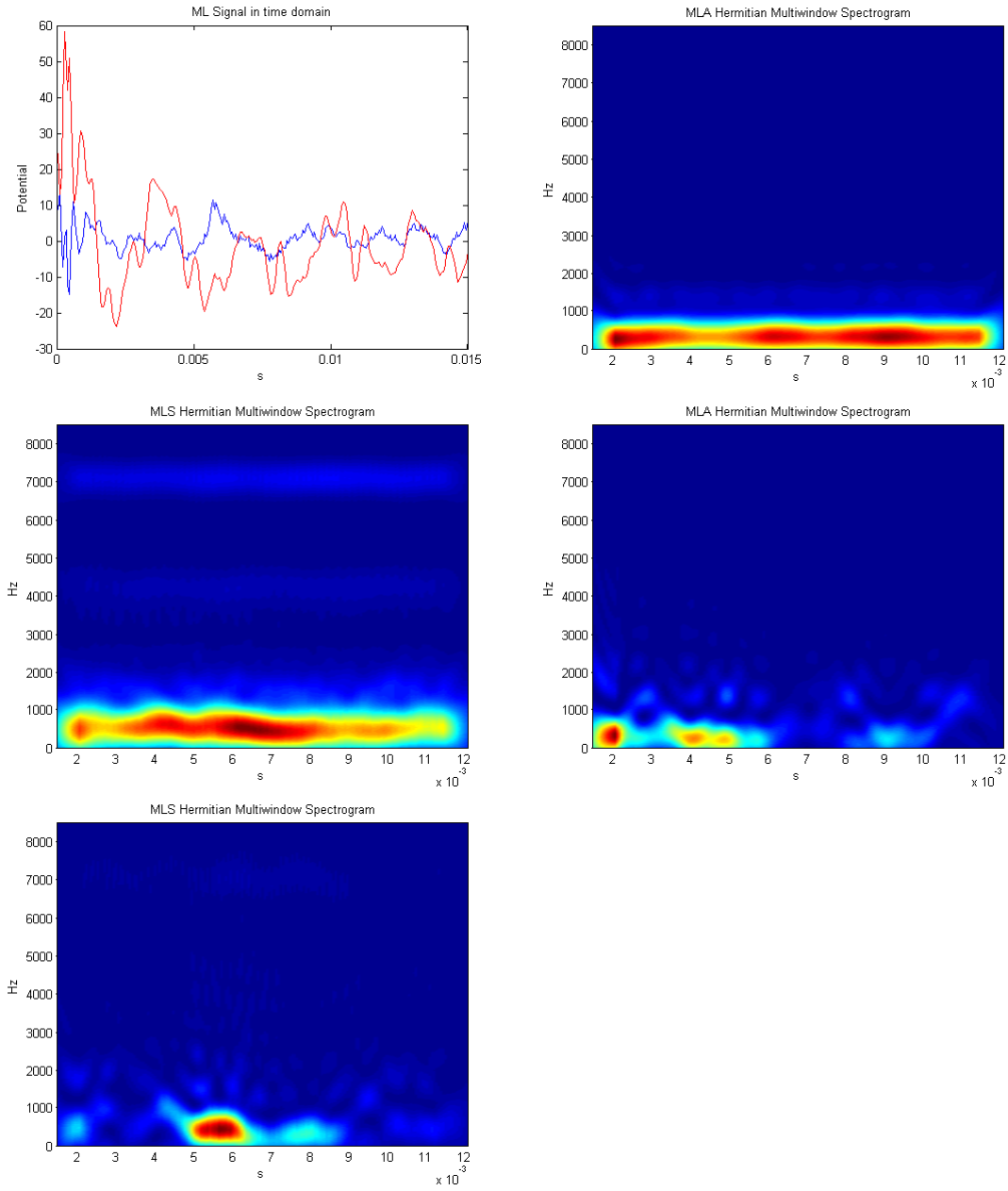

Figure 6.11: Den första plotten visar signalen från patienterna ML. Den röda linjen visar data från varket tillstånd och den blå från sövt tillstånd. De efterföljande plottarna visar spectrogrammet av två olika medelovärdesbildningar för patienten ML. Först för vaket tillstånd och sedan för sövt tillstånd.

Diskussion

Det är ganska tydligt att den slutgiltiga modellen har likheter med den verkliga signalen. De är inte identiska, men de är en bra utgångspunkt om man vill fortsätta att bygga vidare på en mer avancerad modell för hjärnstamssvaret. Om man modifierar vissa parametrar i modellen kan man få en modell som stämmer ännu bättre överens med verkliga data.

Det är väldigt svårt att kvantifiera resultat från en såpass brusig och svår signal som denna, men vi kan se att det sker ett visst latensskift för de tidiga topparna mellan de mätningar som gjorts i vaket tillstånd och i sövt tillstånd. Dessutom ser vi att de senare topparna för det sövda tillståndet tar ut varandra. Mätningar i frekvensdomänen visar på att det trots allt finns en signal där, men den verkar vara ur fas och tar således ut varandra över medelvärdena.